

Itineraries for charging and discharging a BESS using energy predictions based on a CNN-LSTM neural network model in BCS, Mexico



Mario A. Tovar Rosas ^{a,*}, Miguel Robles Pérez ^a, E. Rafael Martínez Pérez ^b

^a Instituto de Energías Renovables (IER - UNAM), Mexico

^b Facultad de Ciencias (FC - UNAM), Mexico

ARTICLE INFO

Article history:

Received 5 August 2021

Received in revised form

2 February 2022

Accepted 12 February 2022

Available online 1 March 2022

Keywords:

Neural networks

Energy predictions

CNN

LSTM

BESS

Energy management

Electric peak shaving

ABSTRACT

Renewable energy generation (REG) is erupting throughout the globe and it points to be the path for a sustainable energy future. Nevertheless, due to their volatile nature, they present a challenge for integrating these intermittent sources into the grid. In this work we present itineraries for charging and discharging two ideal Battery Energy Storage Systems (BESS), one powered with a solar PV generation system and the other one powered with wind energy. Using predictions for REG and electric demand (ED), based on a hybrid Convolutional Long-Short Time Memory (CNN-LSTM) neural network, we propose accurate itineraries to know when to charge and when to discharge variable REG, in the area of Baja California Sur (BCS) in Mexico, pursuing to reduce the ED in peak hours. The convolution net will extract local features and the LSTM the temporal ones. The proposed itineraries of charge and discharge based on predictions with the hybrid CNN-LSTM model, are compared with itineraries made with a well known benchmark and itineraries based on true observations points of REG. The results show that the integration of two BESS with charging and discharging itineraries based on a CNN-LSTM model, can effectively mitigate two important peaks of the electric demand profile in the studied location.

© 2022 Elsevier Ltd. All rights reserved.

1. Introduction

The growing integration of electric power generation systems based on renewable sources implies new challenges to guarantee an efficient, sustainable and safe electricity supply. In this sense, the design of integrated renewable systems in the context of distributed generation (DG) and intelligent Battery Energy Storage Systems (BESS), represent an alternative to face these challenges [1–3]. Depending on the present and future electric demand and generation, different energy storage units, with different storage durations will be required in order to ensure a stable and reliable function of the electricity grid [4,5]. The current main driver for the need of energy storage is the fact that renewable energies in general, and particularly photo-voltaic power generation (PVPG) and wind power generation (WPG), are increasingly entering the electricity market whilst displacing conventional technologies [3].

In this way, a more sustainable and intelligent energy sector is emerging [6]. However, it is important to study and analyze the

intermittent nature of these new generation sources. In this work, the impact of the inclusion of renewable energy sources in a specific electrical power system in Los Cabos San Lucas (LCSL) in BCS is analyzed. On the other hand, BCS's electrical system is isolated from the National Electrical System, so it must satisfy its own electrical demand with local generation, which increases the impact of renewable generation sources *in situ*.

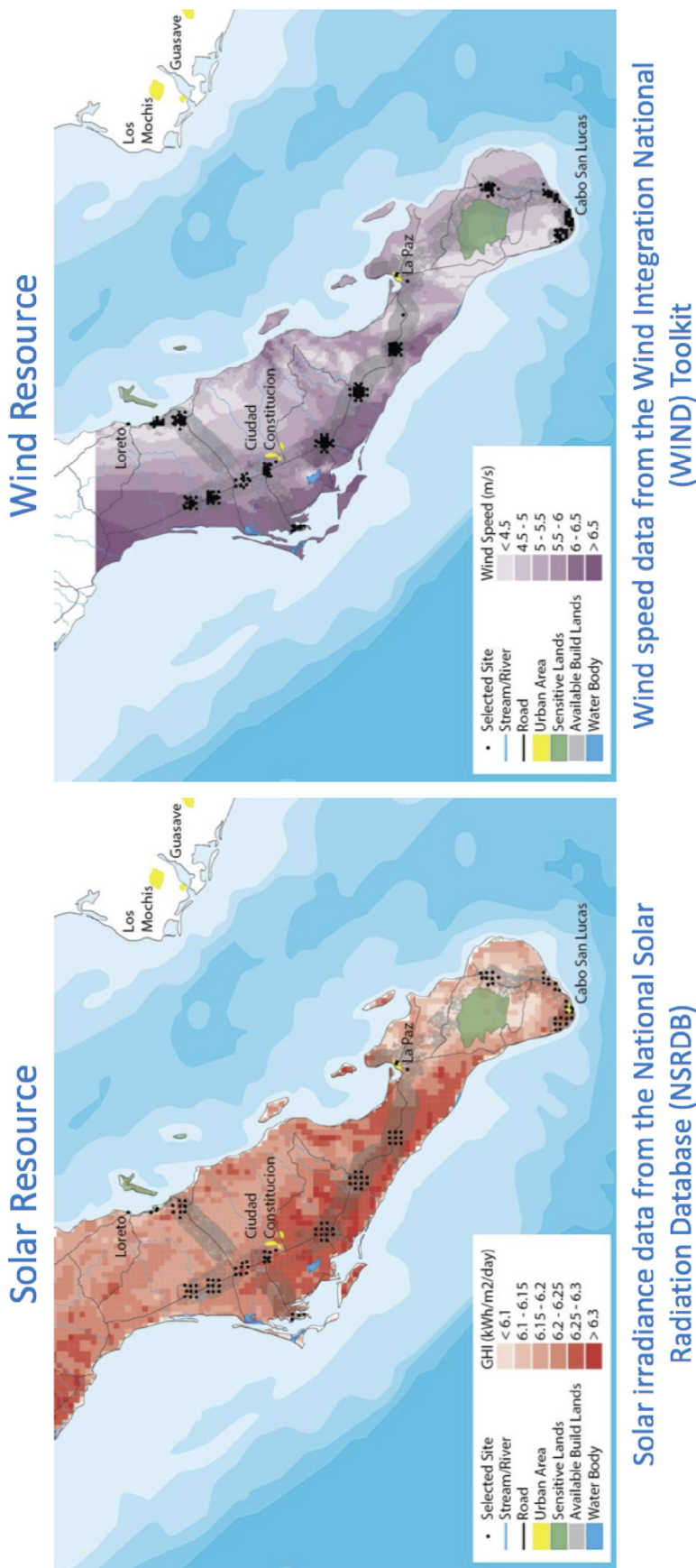
Furthermore, BCS has one of the most polluting electrical generation systems in the country and with high prices in electricity rates [7,8]; The eruption of renewable energies in a joint generation scheme represents an option with great benefits. Due to its characteristics, the BCS area is a place with great potential for the implementation of DG with REG in the state.

In other words, there is a great potential as far as solar and wind energies are concerned; moreover, with an independent electrical system, renewable local energy has high autonomy importance. Some studies, such as the one carried out by the National Renewable Energy Laboratory (NREL) of the United States, presented in 2016 in the framework of the Alliance of Electrical Systems of the XXI Century (21CPP), shows that the BCS area has a great potential for solar and wind energy in particular (Fig. 1) [9].

Considering the characteristics of BCS presented above, it is

* Corresponding author.

E-mail address: matr@ier.unam.mx (M.A. Tovar Rosas).



Wind speed data from the Wind Integration National (WiND) Toolkit

Solar irradiance data from the National Solar Radiation Database (NSRDB)

Fig. 1. Solar and wind resource in BCS [9].

evident that the penetration of electricity generation from renewable sources can represent an important percentage in the region, which would transform the BCS system from being a highly polluting system into a clean, modern and renewable system. For these reasons, it is necessary to carry out studies to incorporate novel techniques like machine learning models, to increase the reliability and penetration of renewable generation systems in the electrical network by trying to reduce local peaks of electric demand with accurate itineraries of charge and discharge. The main objective of this work is to use predictions from a neural network based model, to create itineraries of charge and discharge electricity in a study case where renewable energy come from two sources, and with energy storage, to reduce the energy demand from the electrical grid.

1.1. Predictions - State of the art

In general, there are three main prediction methods: statistical models, physical models and machine learning models. The physical model relies on dynamics between the studied phenomena and physics laws [10]. The statistical model mainly depends on historical data, statistics and probability theory to forecast future time series [11,12]. The machine learning models map directly from inputs to outputs, they extract complex nonlinear features in a very efficient way [13,14]. In the machine learning models we can highlight artificial neural networks (ANN) especially one type of ANN. Recurrent neural networks (RNN), which is one of the most commonly used methods for forecasting time series [15,16]. The RNN has been studied in various applications like wind speed prediction [17], energy power consumption prediction [18–20] or even traffic prediction [21], achieving excellent results.

However, one common problem in RNN (with gradient-based learning methods and back-propagation), is the vanishing of gradient. Gradient vanishing occurs while training long data sequences. This means that the gradient of the loss function approaches zero, making the network hard to train [22]. Long Short Term Memory networks (LSTM) solve this problem [19,23–25].

On the other hand, renewable energy predictions such as PVPG and WPG prediction, has been studied using LSTM models by many authors [13,16,22,26,27] reducing considerably the prediction error compared with other traditional methods.

In recent years, many researchers have combined CNN and LSTM models to extract temporal and spacial features [28–30] achieving accurate predictions in different chaotic phenomenons. In the medical field for example, Gill et al. proposed a CNN-LSTM model to accurately detect arrhythmias in electrocardiograms [15]. For ED prediction, some authors [31–33] proposed a hybrid CNN-LSTM model for electric energy consumption achieving superior results than other deep learning based methods. They found that time series decomposition with deep learning models provides useful visualizations to better understand the problem of predicting and analyzing energy consumption [31].

Wang et al. proposed an hybrid LSTM-CNN model for PVPG prediction [34]. They introduced a hybrid model of one dimension for PV prediction. In 2020, Other authors [35,36] proposed a similar hybrid CNN-LSTM model with a stronger multi-layer architecture, this includes a 5D-CNN model with max pooling and a 5D-LSTM model. Indeed, the five dimensional CNN-LSTM model consume more computational resources for training than an uni-dimensional model, but high accuracy was achieved [35,36]. Other authors with similar machine learning techniques had achieved excellent results [37–39], we need to remark that this work is not a comparative between other machine learning techniques, but with a well known benchmark.

1.2. BESS and peak Shaving

In this section we will present the state of art of BESS technologies and the implication of using these systems for peak reduction in the studied area.

Electrical energy storage systems (EESS) are often entirely and exclusively associated with energy shifting, for example, the matching of generation with consumption, as their only or principal role in the electric grid. However, these systems are not limited to just that application, they also can provide a broad variety of stable, reliable and economic function to the electricity grid [3,4]. The EESS can be divided by their storage technology, as it is shown in [Table 1](#).

Many articles that show the state of the art of EESS, compare the efficiency of different storage type units [40], and in the case of electrochemical storage units, they compare the efficiency of different materials [9]. In this work we will idealize a BESS, because the state of the art shows better performance of electrochemical technology compared with mechanical or thermal storage [3,40]. We also emphasize the need to incorporate machine learning techniques based on data, for having an accurate energy management of intermittent energy sources in storage systems. In other words, machine learning techniques, specially hybrid neural networks models, can give accurate predictions [4,27,41], to decide when to charge and when to discharge the energy.

On the other hand, we will propose a peak shaving method for a particular case of study: Los Cabos San Lucas in Baja California Sur (LCSN-BCS). As we will expose in the third chapter, the electrical grid of BCS have several turbo-gas generators. Which are often used to match the electricity consumption in the peak demand hours, but are highly pollutant and expensive [42]. If we could use a cleaner source like solar or wind energy, it will impact directly in the pollution due to the use of these contaminant generators.

So, controllability of BESS will provide enhanced flexibility to the BCS system. However, in order to interact with the grid dynamically, and improve the coordination, which will lead to peak demand reduction and energy saving, new technologies as smart devices, bi-directional communications and integrated management need to be integrated [1,43,44].

2. Baja California Sur case of study

2.1. Solar resource in BCS

In this section we will use weather data to estimate the solar resource in the BCS area, and then simulate a PVPG plant. To assist us in this process, we will use the free license software: System Advisor Model (SAM) from NREL [45,46].

The irradiance profile throughout 365 days in BCS, in the studied location (the latitude and longitude are shown below), which correspond to the city of Cabo San Lucas, is shown in [Fig. 2](#) (raw data). As it can be seen, the months of March, April and May are the months where there is a much greater value of irradiance. In counterpart, the smallest irradiance values are in the months of December and January. Note that the variation can go from 200[W/m²]

Table 1
Overview of EESS [3,4,40].

Storage	Medium examples
Electrical	Super-capacitors and inductors
Mechanical	Flywheels, Compressed Air Energy Storage (CAES) or Pumped Hydro
Thermal	Phase change materials and thermochemical energy storage
Electrochemical	Redox-Flow batteries, Lead-Acid batteries or Lithium-Ion batteries

m^2] to maximum values of $1100[W/m^2]$, this is one of the great disadvantages and challenges of solar energy, the intermittent nature of solar irradiance.

LATITUDE = 22.972 185

LENGTH = -109.667 267

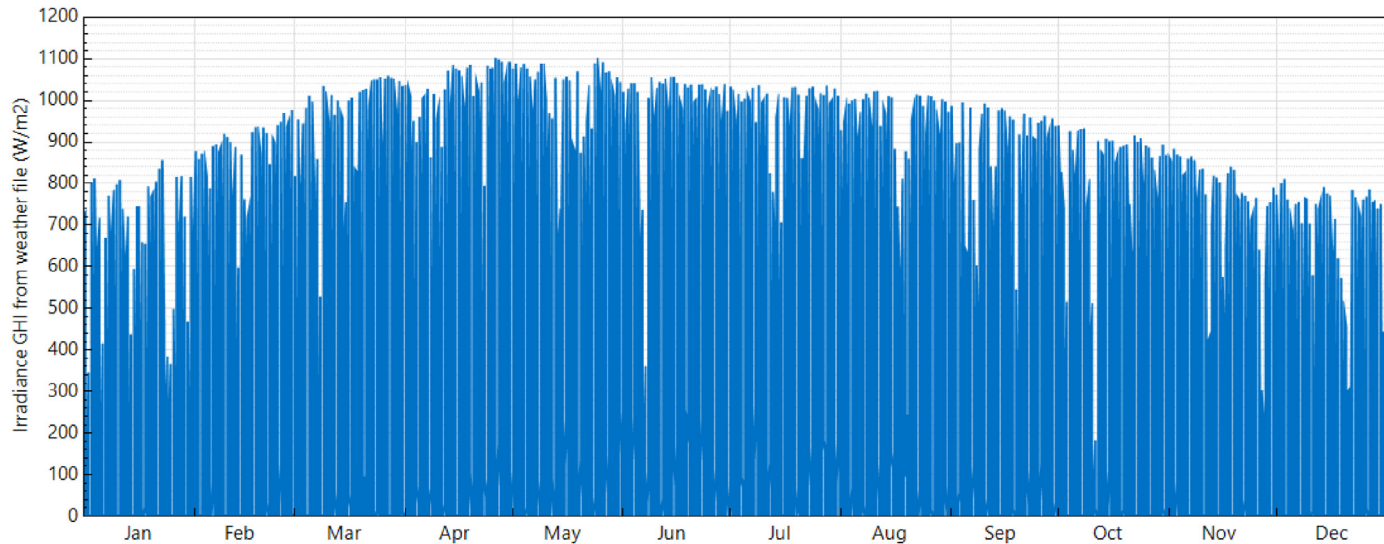


Fig. 2. Global irradiance in BCS during 2018 [45,46].

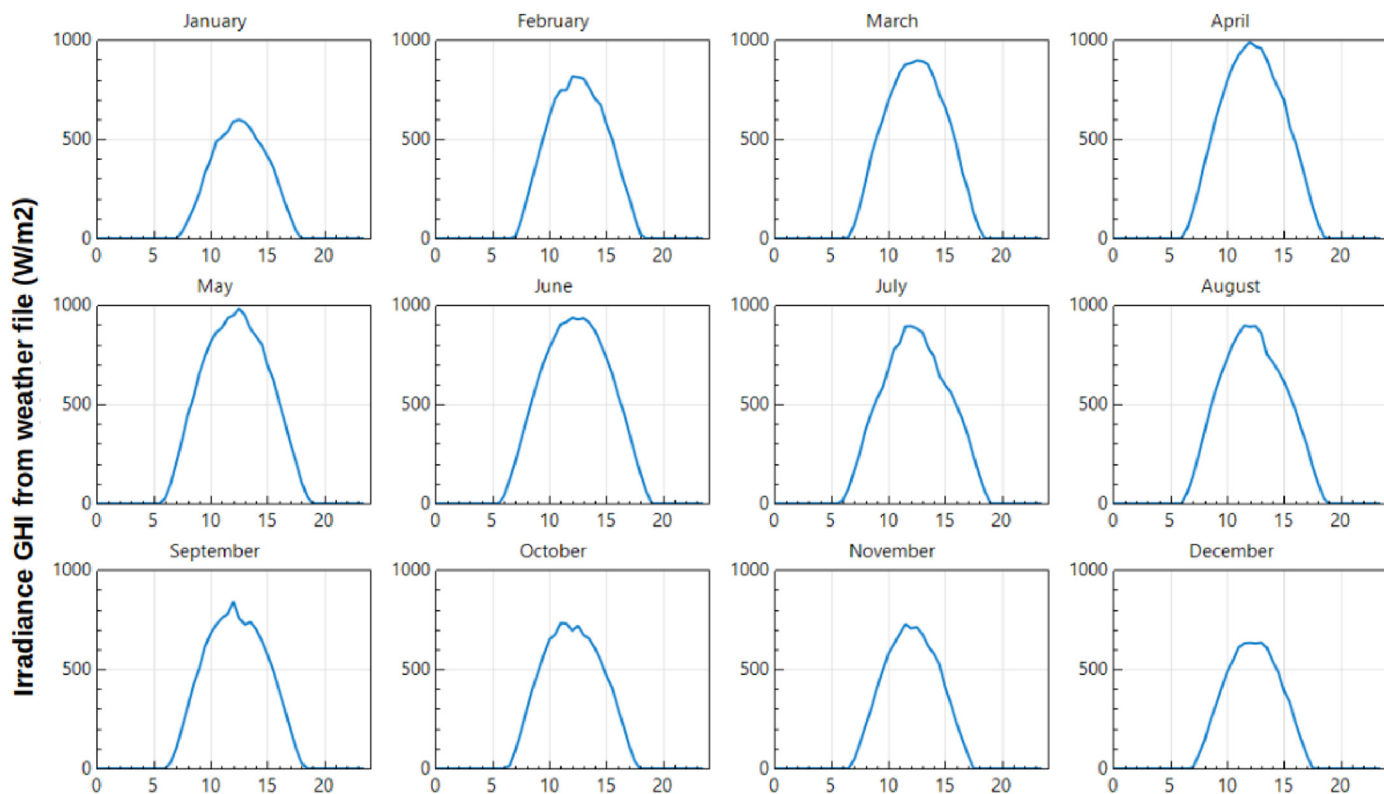


Fig. 3. Irradiance avarage profiles by month in BCS [45,46].

2.2. Wind resource in BCS

As we did with the solar resource in the last section, we will use SAM and the wind velocity data files corresponding to the coordinates of Los Cabos San Lucas, to simulate a wind generation plant (Fig. 6). As we can see in Figs. 4 and 5, the wind resource is abundant in the region throughout the hole year. Nevertheless the volatile nature of wind resource is considerably big. As we can observe in Fig. 4, wind speed can variate from 0 – 18[m/s].

The specifications of the wind turbine are: ElectriWind Garbi 140 [kW] wind turbine (fabricator), hub height = 80 mts, shear coefficient = 0.13. In Fig. 6 we can highlight that the wind speed cut in is at 2[m/s] and the wind speed cut off the turbine is at 14[m/s], taking a good advantage of this variant source. In Fig. 5 the wind average velocity per month is shown. We can highlight that mostly there is abundant wind resource in nigh time hours and an important decrease from 10:00 to 15:00. However for the solar case, these are the hours of high irradiance (Fig. 3), this is why we propose a solar-wind hybrid generation in LCSN-BCS area.

2.3. BCS electric grid

The BCS zone contains an autonomous electrical system that is isolated from the national electrical network, as it is shown in the transmission map of the Mexican national territory (Fig. 7). The BCS system is made up from two systems: Mulegé (53) in the northern part of the state, and BCS in the southern part (50–52), where the centers with the largest loads are located (La Paz, San José del Cabo and Cabo San Lucas) [7,42].

Baja California Sur's electrical system is divided in three regions: Constitución, La Paz, and Los Cabos. The map in Fig. 8 shows a general diagram of this transmission system, including the three electrical zones of the BCS's system and the location of the main load centers and generation plants. As it can be seen in Fig. 8, there are currently 28 consumption centers, 2 internal combustion plants, 3 turbo-gas, 1 thermal-electric, 1 combined cycle, 1 wind farm and 3 photo-voltaic solar plants, adding a total installed capacity of 883,805 MW [42].

Moreover, some studies demonstrate that the incorporation of BESS powered with REN can effectively decrease peaking power plants [47,48], if a good energy management system is incorporated [49]. The region of BCS is highly gifted with solar and wind resource [9], therefore in this work, a hybrid neural network based novel technique for scheduling itineraries of charge and discharge is proposed, to incorporate a data based energy management of renewable variable sources in a specific region of LCSN-BCS.

3. Ideal model of a Battery Energy Storage System (BESS)

The aim of the BESS model is to maximise the percentage morning and evening peak reduction for the demand on a primary and a secondary distribution feeders for each day over a five days period, whilst utilising as much solar PVPG or WPG as possible to do so.

This is done by finding an appropriate charging profile for the storage device so that it charges at the correct rate during daytime periods (or night time periods) when there is high solar or wind generation, and discharges at the correct rate during certain period in the morning or in the evening. This is done the following way. First, the battery storage device is limited by the maximum import and minimum export rate of charging and discharging respectively.

$$B_{min,le}; B_{d,kle}; B_{max} \quad (1)$$

Where, for this work the maximum charge rate is $B_{max} = 50$ kW

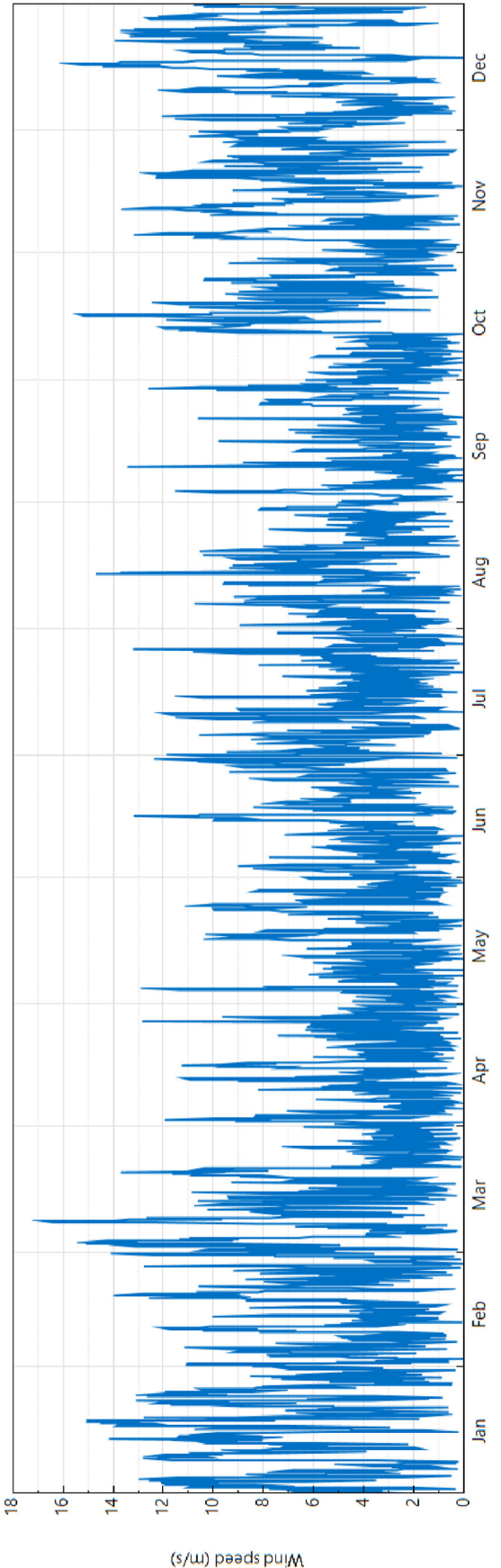


Fig. 4. Wind speed profile in BCS [45,46].

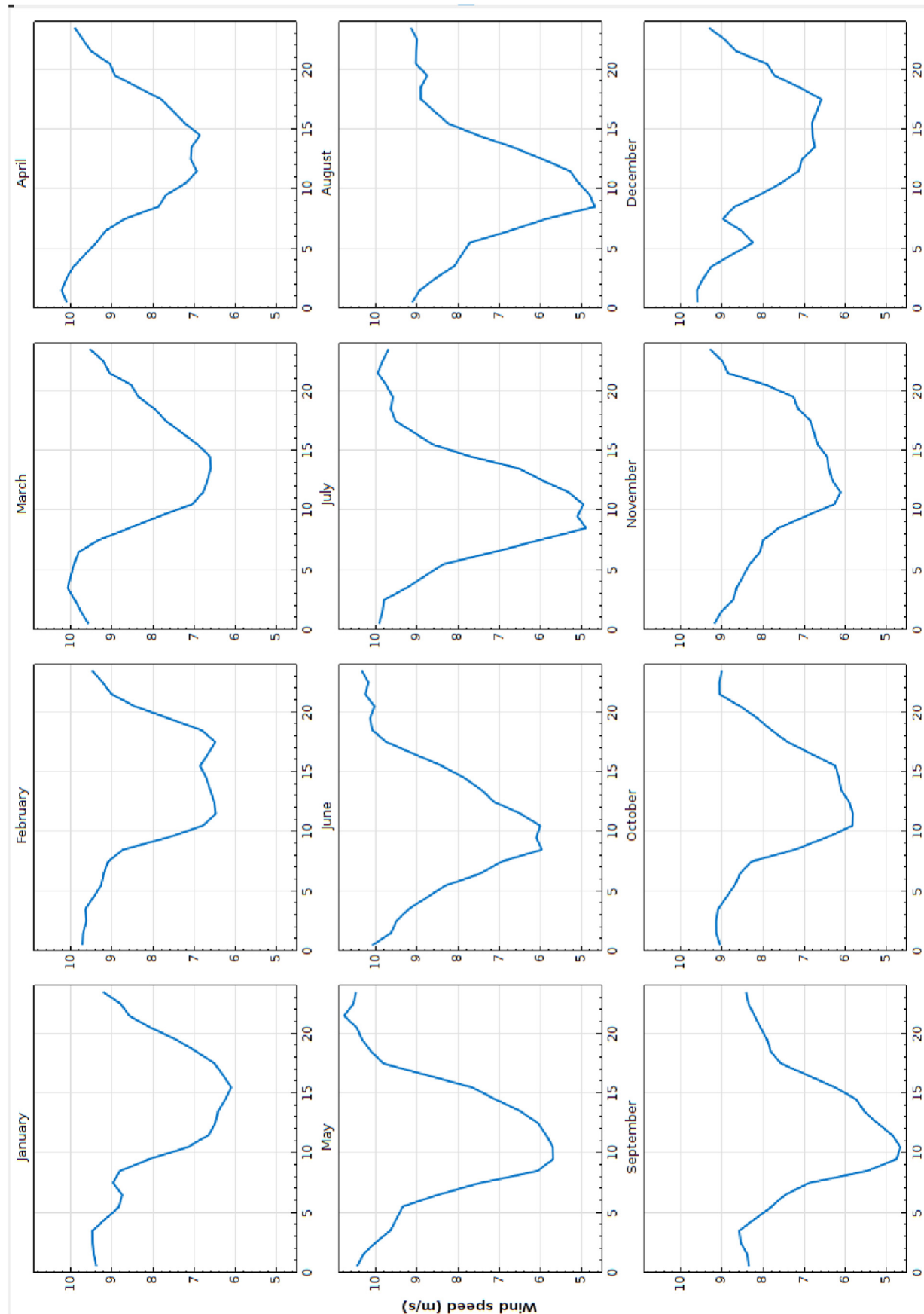


Fig. 5. Wind average profiles by month in BCS [45,46].

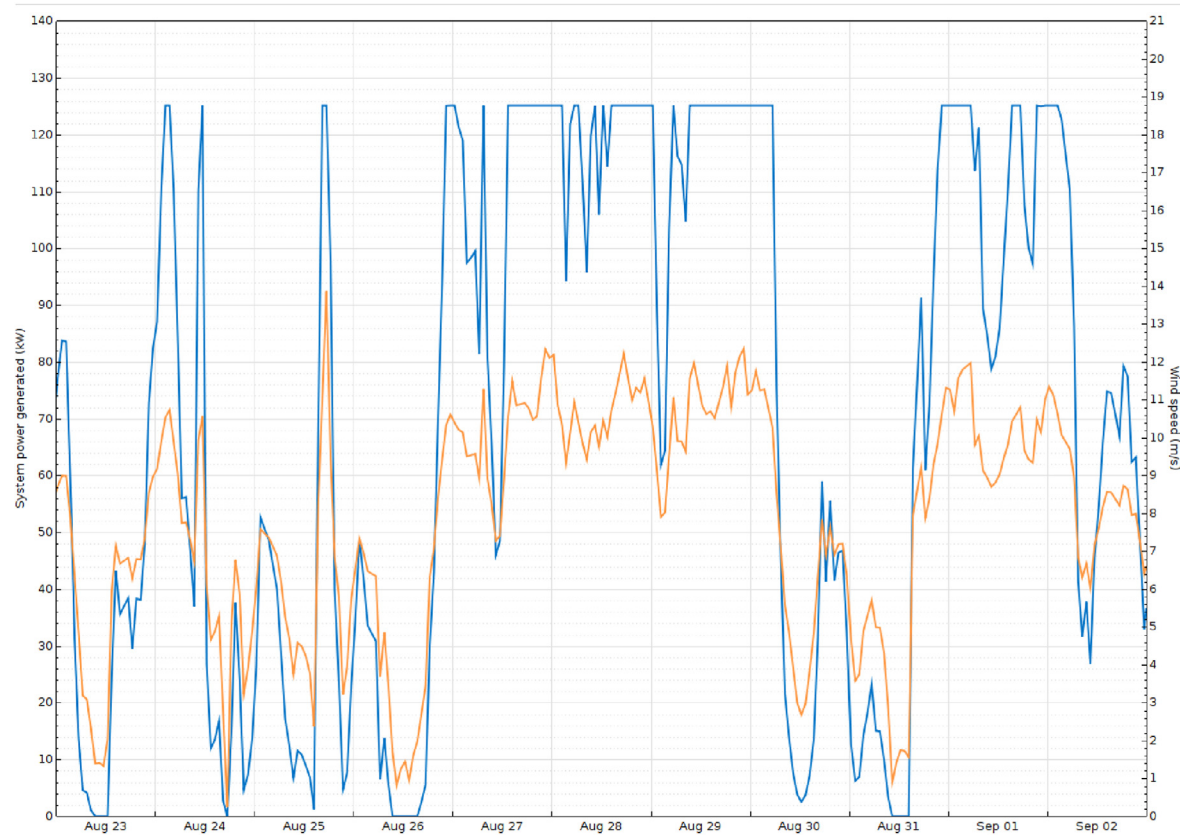
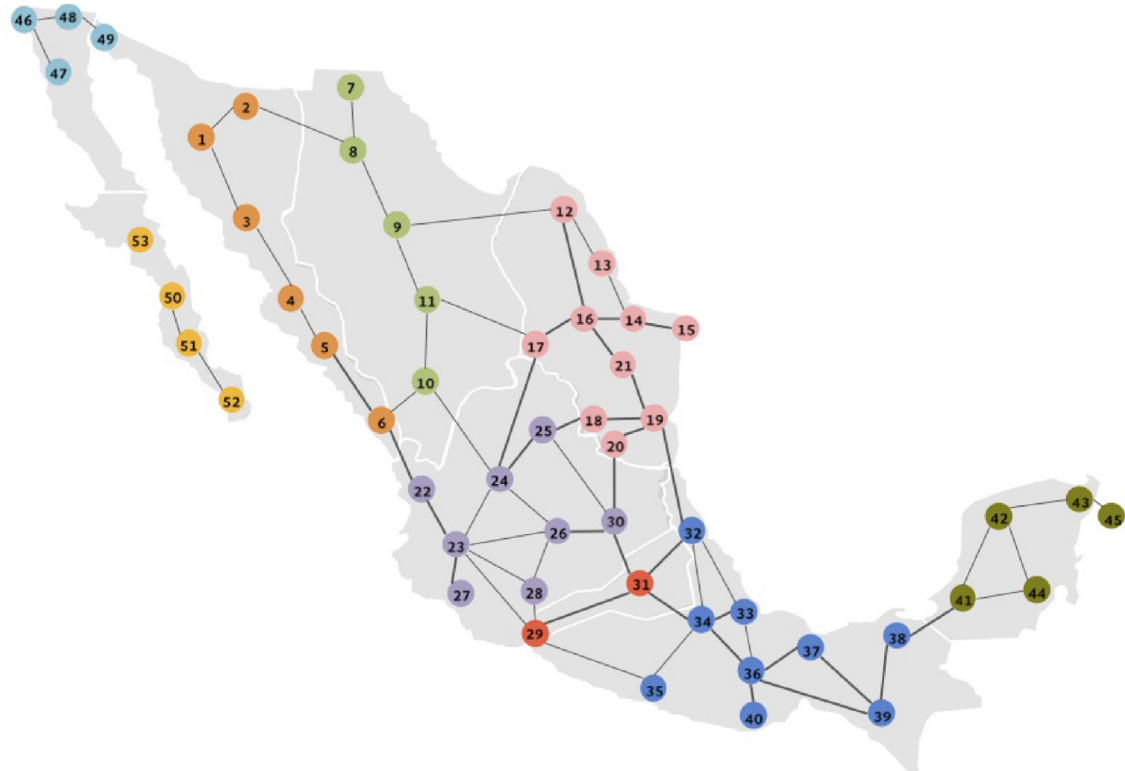


Fig. 6. Wind speed and SPG by a 140 kW turbine in BCS [45,46].



Fuente: Elaborado por la SENER con información del CENACE.

Fig. 7. Electric systems in Mexico [42].

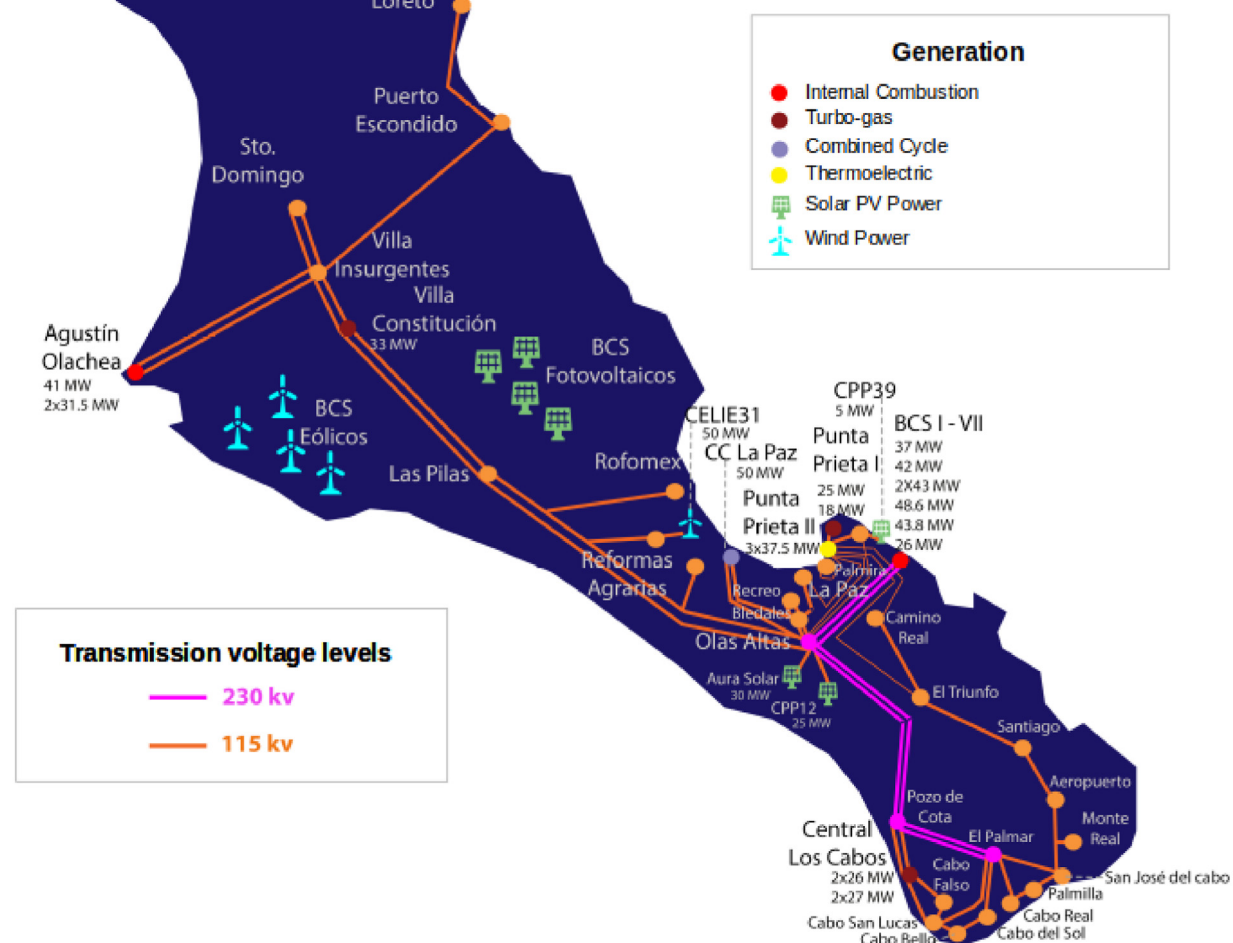


Fig. 8. BCS Electrical grid system [7,42].

and the maximum discharge rate is $B_{min} = -50$ kW. Secondly, the battery cannot charge beyond its capacity. Let $C_{d,k}$ represent the total charge (in KWh) in the battery on day d and half hour k, and so.

$$0 \leq C_{d,k} \leq C_{max} \quad (2)$$

Where the maximum capacity for this work is $C_{max} = 500$ KWh. The change in the total charge in the battery from one step to the next is related by:

$$C_{d,k+1} = C_{d,k} + 0.5B_{d,k} \quad (3)$$

The other aim of the BESS is to maximise the amount of PVPG or WPG. In other words, when $B_{d,k} \geq 0$, (i.e. when importing) then the charge can be written as:

$$B_{d,k} = P_{d,k} + G_{d,k} \quad (4)$$

Where $P_{d,k}$ is the average power stored in the battery from the renewable source and $G_{d,k}$ is energy stored from the grid at hour k.

If the remaining capacity of BESS ($C_{d,k}$) is less than the minimum discharge rate during the peak load, it will discharge the total remain capacity.

Finally the performance of the ideal BESS proposed model with PVPG is shown in Fig. 9, as it is expected the charge rate starts increasing with the PV generation, and starts decreasing (discharging) during the selected time window during the afternoon.

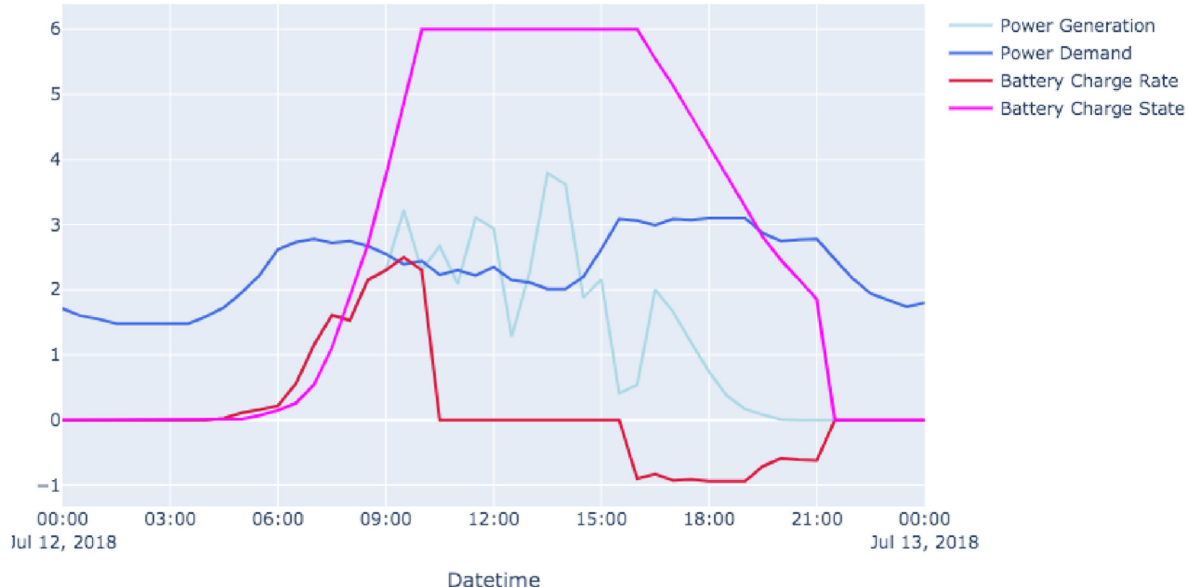
For the mexican legislation [50], distributed generation is considered when the system power generated is less than 500 [kW], for more than 500 [kW], the local marginal price (PML) should be considered in the battery charging and discharging strategy.

4. The dataset and the CNN-LSTM neural model

In the next sections we are going to present the data used for training the proposed hybrid model. As well, the CNN and the LSTM models themselves will be introduced.

4.1. Weather variables in BCS

In this section the weather dataset is presented, in Fig. 10 the variables from the NREL dataset from the studied location, Los Cabos San Lucas, BCS is presented. This includes six variables measured throughout 2018 such as: Global Horizontal Irradiance

**Fig. 9.** Ideal BESS charging with PVPG.

(GHI in $[W/m^2]$), which is composed by the Diffuse Horizontal Irradiance (DHI in $[W/m^2]$) and the Direct Normal Irradiance (DNI in $[W/m^2]$). We also include the wind speed profile of the location ($[m/s]$), the temperature ($[^\circ C]$) during the studied year in the region and the atmospheric pressure ($[mbar]$).

4.2. Renewable generation and demand time series in BCS

In this section, we will introduce the electric variables such as: LSCN electric demand, PVPG and WPG (see Fig. 11).

As it was mentioned in Chapter 2, for the PVPG and WPG we use the software SAM [46] from NREL to simulate a 110 [kW] PV plant and a 140 [kW] nominal wind generation plant in the region of LSCN-BCS, México.

For the electric demand (Fig. 12) we use data from the Electricity Federal Commission in Mexico (CFE) of certain hotel industry in the region. As we can see, there is a notorious seasonality trend due to the tourism industry in the months of June, July and August. Also, it is observable that the demand profile has two peaks, one during the morning and the second during night time hours.

4.3. Local feature learning with CNN

CNN are very popular for extracting local features in image processing [51]. Convolution is the main concept of a CNN. Our proposed CNN includes two parts: the convolutional layers (Eq. (5). and Eq. (6).) and the pooling layer (the main purpose of this layer is to reduce the number of parameters of the tensor by reducing its size Fig. 13), therefore this pooling layer helps to decrease computation time.

In the convolution layer, the previous layer features graph interacts with the convolutional kernel; this interaction forms the output feature graph j of the convolutional layer. Each one of this output feature graph j might contain a convolution with multiple input feature graphs. The equations that define the convolution layer are:

$$y_j^{(l)} = \left(\sum_{i \in c_j} t_i^{l-1} \otimes w_{ij}^{(l)} \right) + b_j^{(l)} \quad (5)$$

Where c_j is a set of input feature graphs. b_j^l is the bias, y_j^l the output of the convolution and $w_{ij}^{(l)}$ the convolution kernel.

$$t_j^l = f(y_j^{(l)}) \quad (6)$$

t_j^l the feature graph of the convolution layer l .

$$f(x) = \max(0, x) \quad (7)$$

f is known as the activation function. In this work we use a rectified linear unit (Relu) as f , the activation function.

The core of the convolution feature extraction works by reducing the number of features in a dataset. These new reduced set of features should then be able to summarize most of the information contained in the original set of features. In this way, a summarized version of the original features [29,31,35].

As we will see in Chapter 4.5, feature extraction of the hybrid model works like this: First of all, the upper layer of CNN-LSTM consists of CNN. The CNN layer can receive various variables that affect the studied phenomena, such as the weather variables in our case. Therefore CNN consists of an input layer that accepts multi-variables as inputs, and an output layer that extracts features to LSTMs, and several hidden layers. Then LSTM can extract complex features among multiple variables and that can store complex irregular trends in time. In other words, after training, each weight of the CNN-LSTM model will correspond to a certain input.

4.4. Temporal feature learning with LSTM

The lower layers of the proposed model are the LSTM. This layers store time information about important characteristics of the time series extracted by the CNN. LSTM preserves long-term memory by using memory units that can update the previous hidden state. This functionality makes it possible to understand temporal relationships on a long-term sequence. Its internal

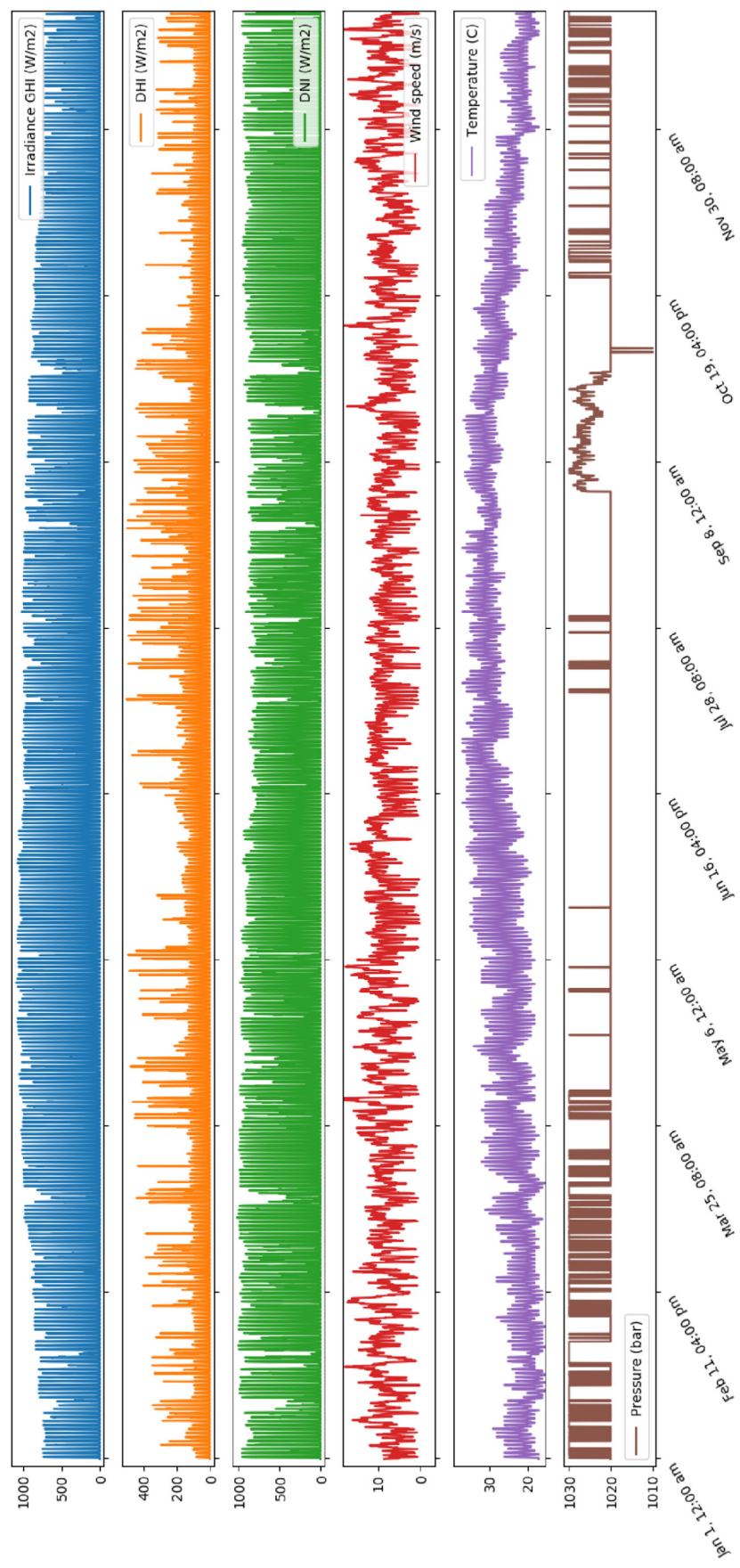


Fig. 10. Weather variables in Los Cabos San Lucas, BCS [45].

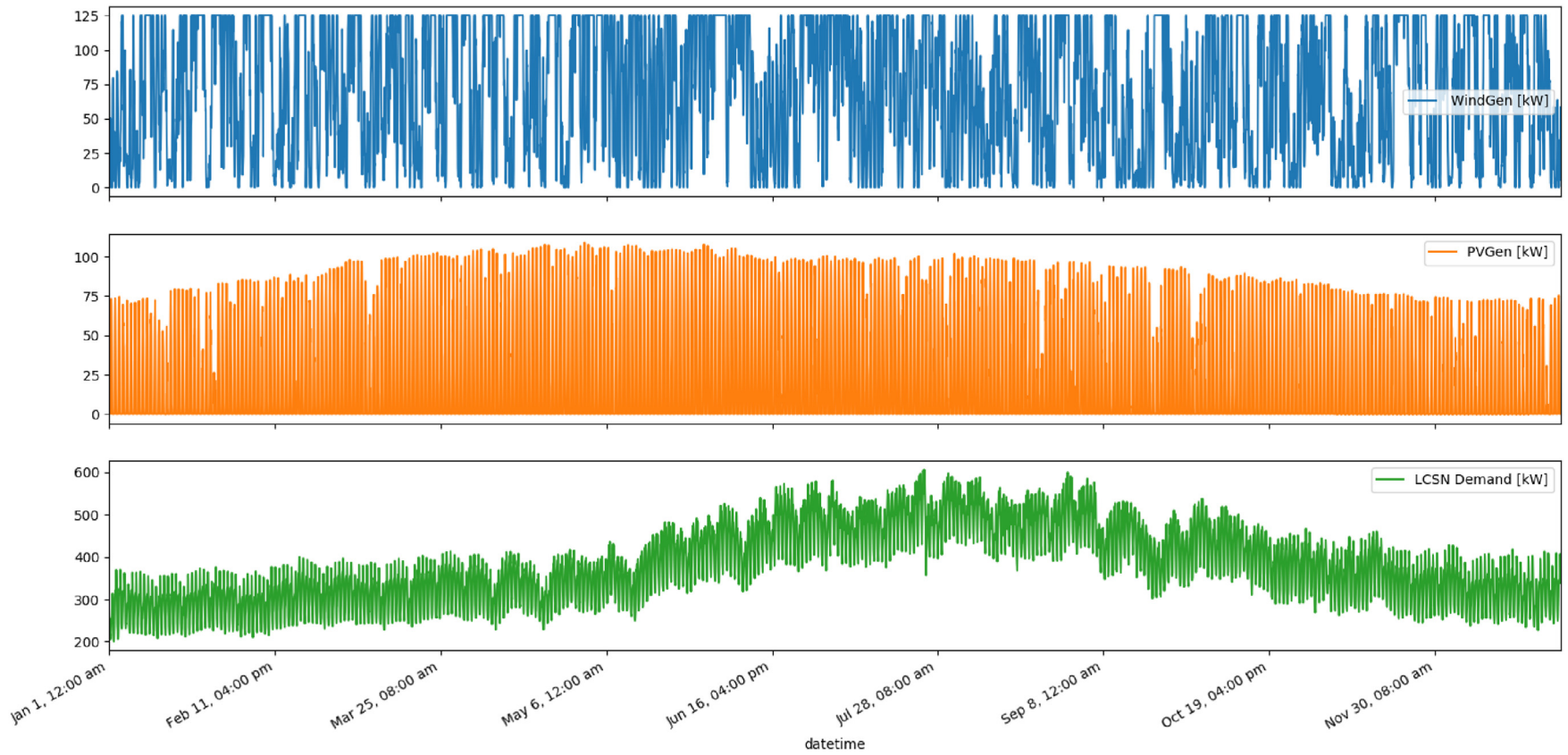


Fig. 11. Renewable generation (WindGen and PVGen) and electric demand in Los Cabos San Lucas, BCS (LCSN-BCS Demand).

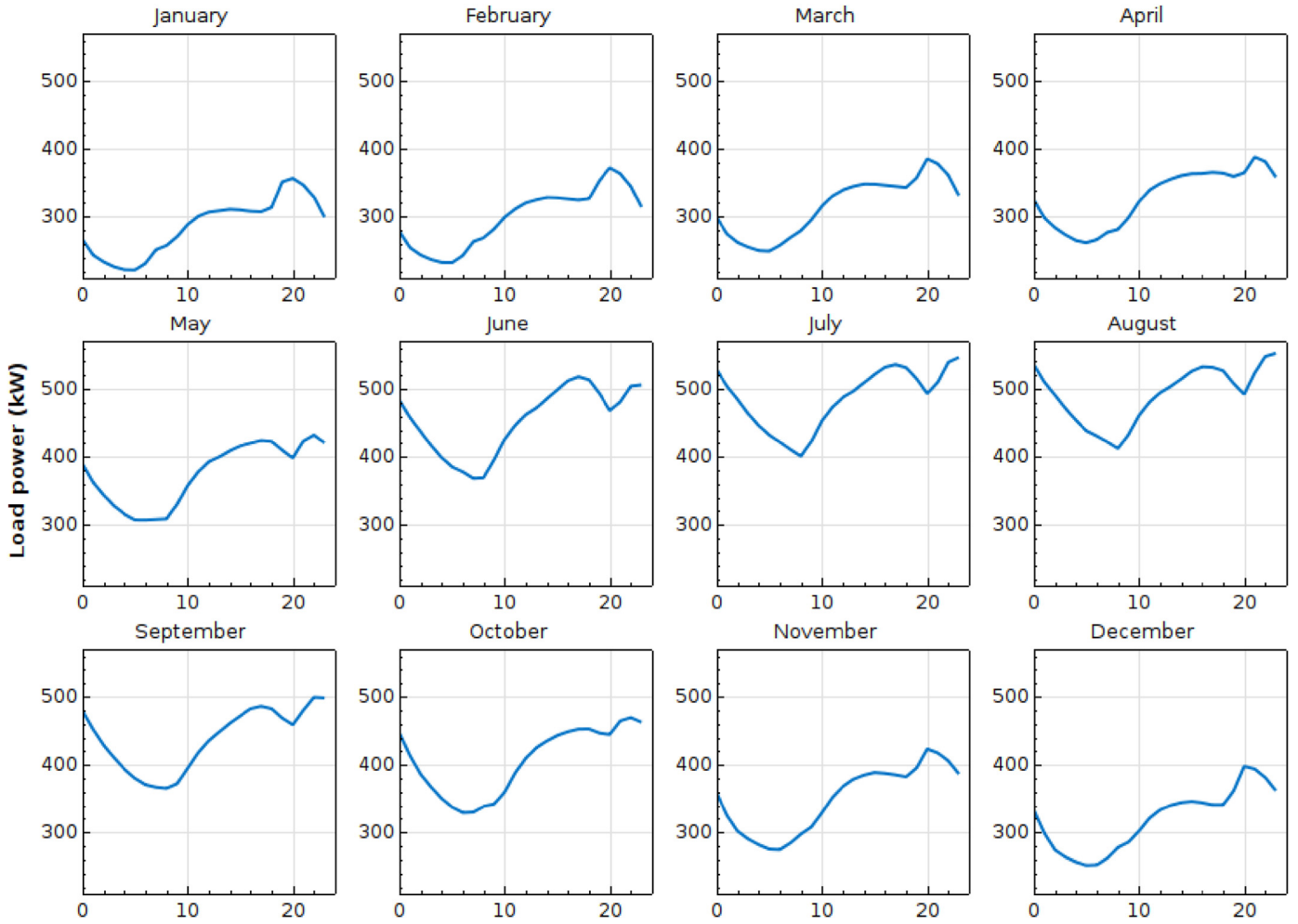


Fig. 12. Demand average profiles by month in Los Cabos San Lucas, BCS.

memory unit and gate mechanism overcome the gradient disappearance problem that occurs in training traditional recurrent neural networks (RNN). The memory channel and the gate mechanism (which includes: forget gate, input gate, update gate and output gate) are shown on Fig. 14. The equations of the LSTM model are the following [25]:

$$f_t = \sigma(W_f \bullet [h_{t-1}, X_t] + b_f) \quad (8)$$

f_t is the output value of the forget gate. And σ refers to the sigmoid activation function.

$$i_t = \sigma(W_i \bullet [h_{t-1}, X_t] + b_i) \quad (9)$$

i_t is the output value of the input gate.

$$g_t = \tanh(W_g \bullet [h_{t-1}, X_t] + b_g) \quad (10)$$

g_t is the output value of the update gate.

$$c_t = f_t * c_{t-1} + i_t * g_t \quad (11)$$

c_t refers to the memory cell.

$$o_t = \sigma(W_o \bullet [h_{t-1}, X_t] + b_o) \quad (12)$$

o_t is the output value of the output gate.

$$h_t = o_t * \tanh(c_t) \quad (13)$$

Where h_t is the output vector result of the memory cell at time t (see Fig. 14). $W_{f,i,g,o}$ are the weights matrices and $b_{f,i,g,o}$ the bias vectors.

4.5. CNN-LSTM hybrid model

The proposed CNN-LSTM structure as it is shown in Table 1, it consists of three dimensional CNN and LSTM structures and a fully connected layer. The input of the neural network has ten variables, such as temperature, irradiance, wind speed and others (see subsection 4.1 and 4.2 for more information about the variables).

First, the upper layer of CNN-LSTM consists of a convolutional neural network (CNN). The CNN layers can receive various variables that affect any time series phenomena. On the other side, the dataset is separated in two parts: 80% for training the model and 20% to validate the results.

The CNN consists of an input layer that accepts weather and electric variables as inputs, an output layer that extracts features to LSTMs, and several hidden layers. Fig. 15 for WPG prediction, Fig. 16 for PVPG prediction and Fig. 17 for ED. The hidden layers used consists of: a convolution layer, a ReLU layer, an activation function, or a pooling layer.

From the presented data in the input a unique output pattern is

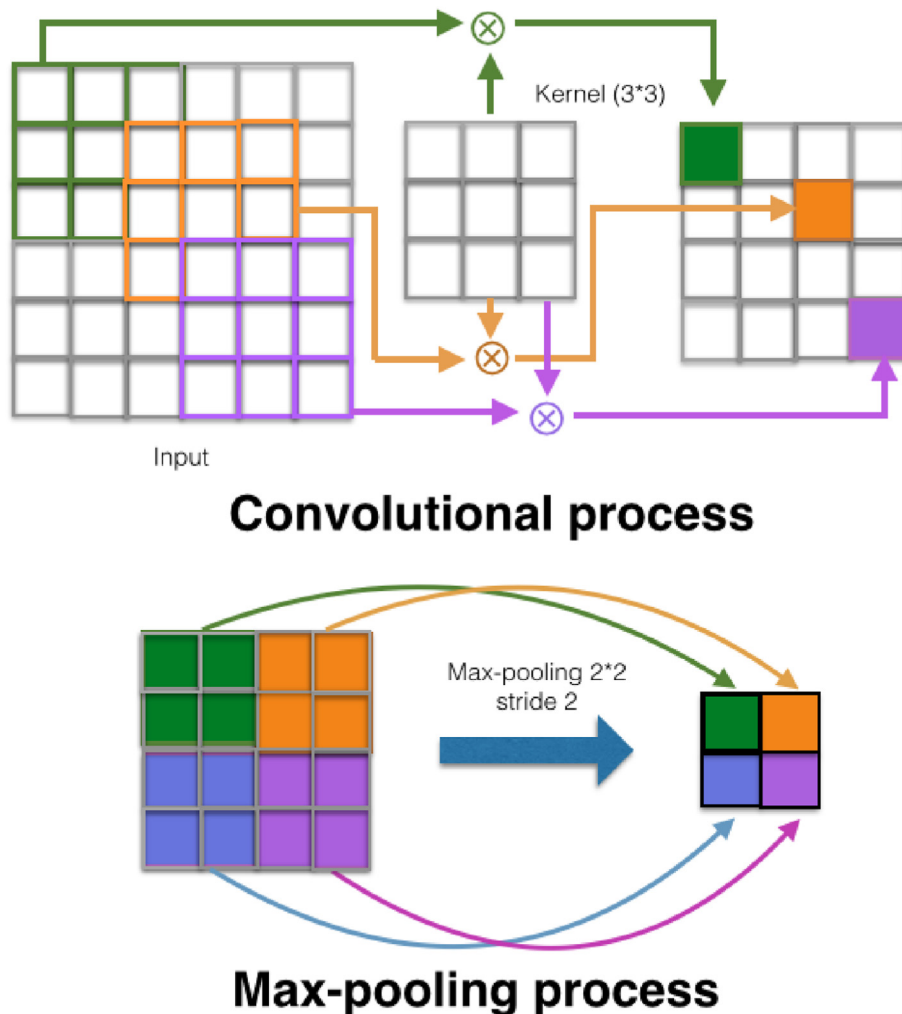


Fig. 13. Convolution and Max-pooling process, image adapted from Ref. [34].

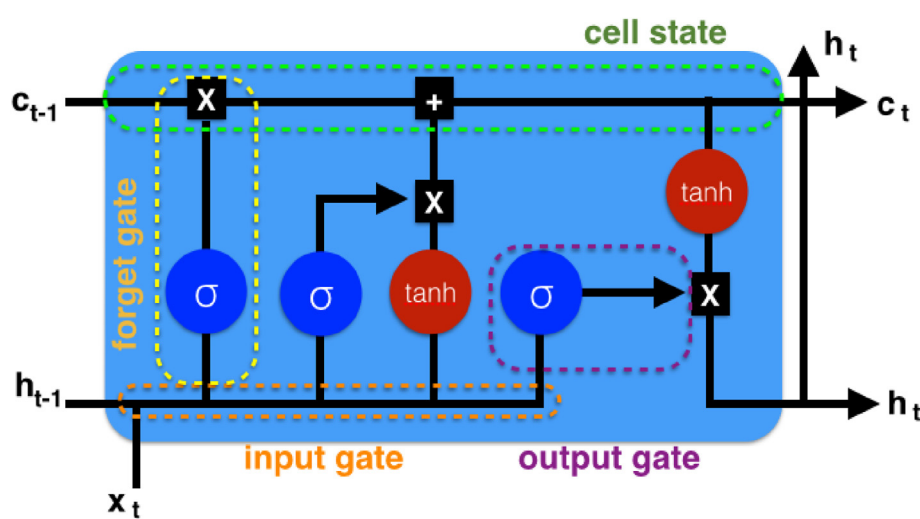


Fig. 14. LSTM cell.

generated. The CNN extracts the local features and the LSTM temporal part. With this structure, the neural network "learns" for every input a weight that determines a specific output.

The CNN configuration in the hybrid model mainly consists of

three convolutional layers and three pooling layers. The number of convolution kernels is 64, 128, and 64 respectively with a ReLU activation function.

The LSTM model in the hybrid model contains five hidden

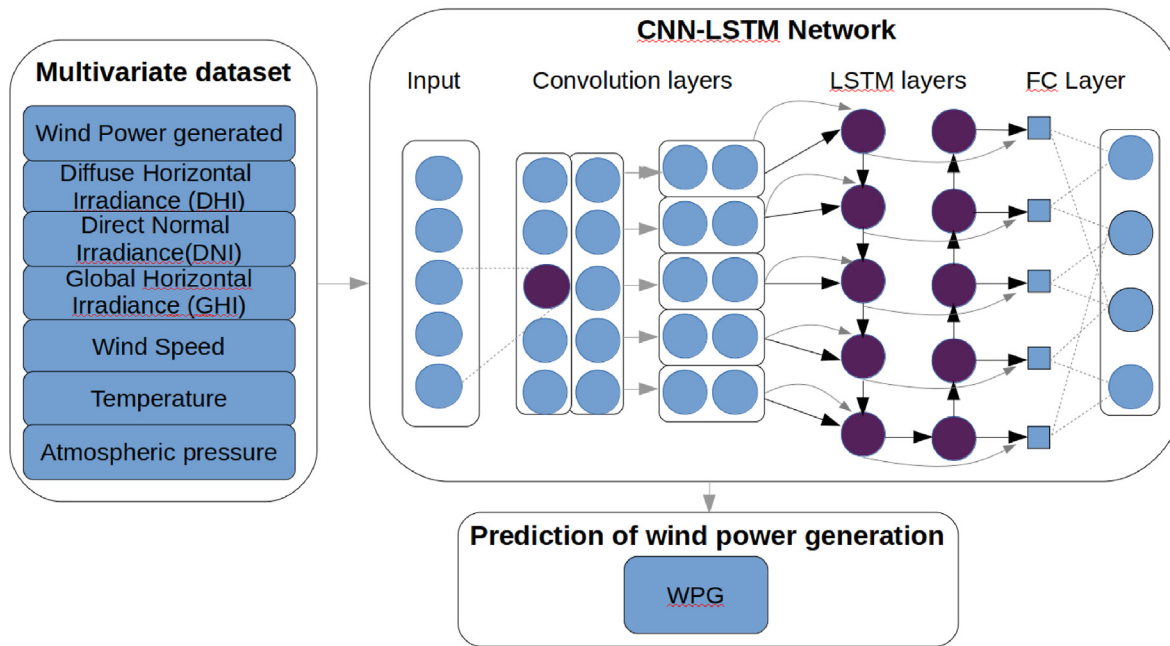


Fig. 15. The CNN-LSTM general structure for the WPG model.

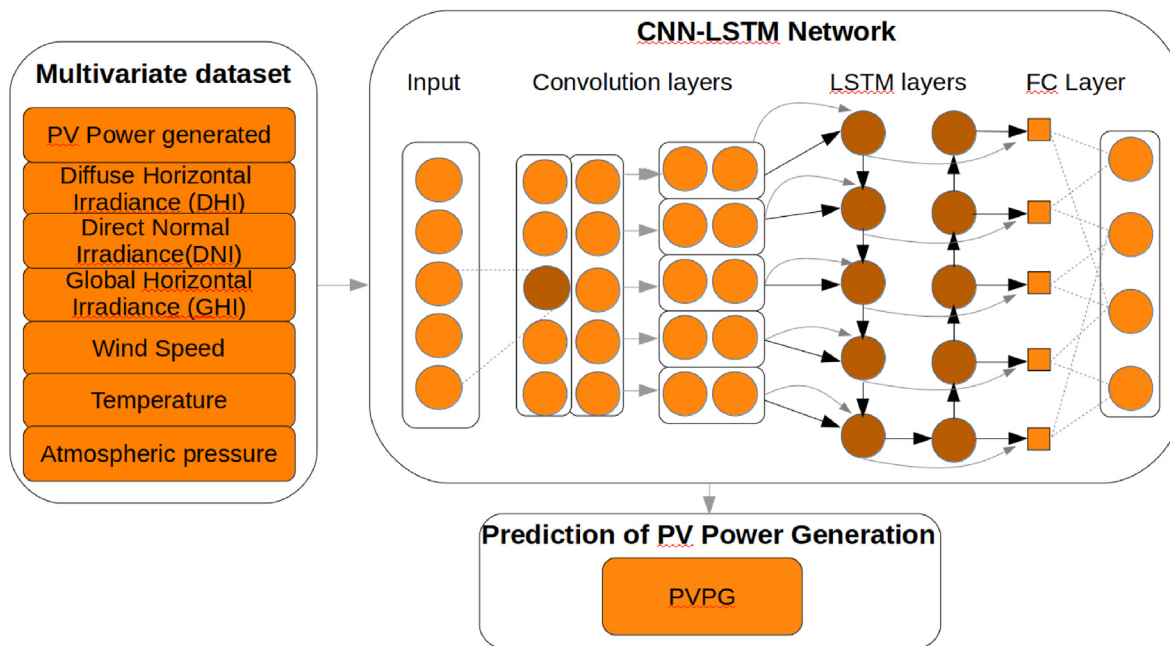


Fig. 16. The CNN-LSTM general structure for the PVPG model.

layers, having respectively 64, 128, and 64 neurons. Finally, there is a dropout of 0.1 to prevent overfitting and finally two fully-connected layer with 1024 neurons. For this experiment 700 epochs were selected. The specific parameter settings of the model are shown in Table 2.

All the hyper-parameters were designed by the trial and error method. This process means that certain hyper-parameters are specified, then trained with 80% of the data and validated with other 20%, for the four seasons throughout the year. Hyper-parameters are then changed and the process is repeated until they are finally optimized.

The proposed model was trained in a multi-step autoregressive modality. In a multi-step prediction, the model needs to learn to predict a range of future values. Thus, unlike a single step model, where only a single future point is predicted, a multi-step model predicts a sequence of the future values. There are two rough approaches to this: Single shot predictions, where the entire time series is predicted at once. And an autoregressive prediction, where the model only makes single step predictions and its output is fed back as its input (Fig. 18). The advantage of this style of model is that it can be set up to produce output with a varying length [52].

In order to demonstrate the good performance of the proposed

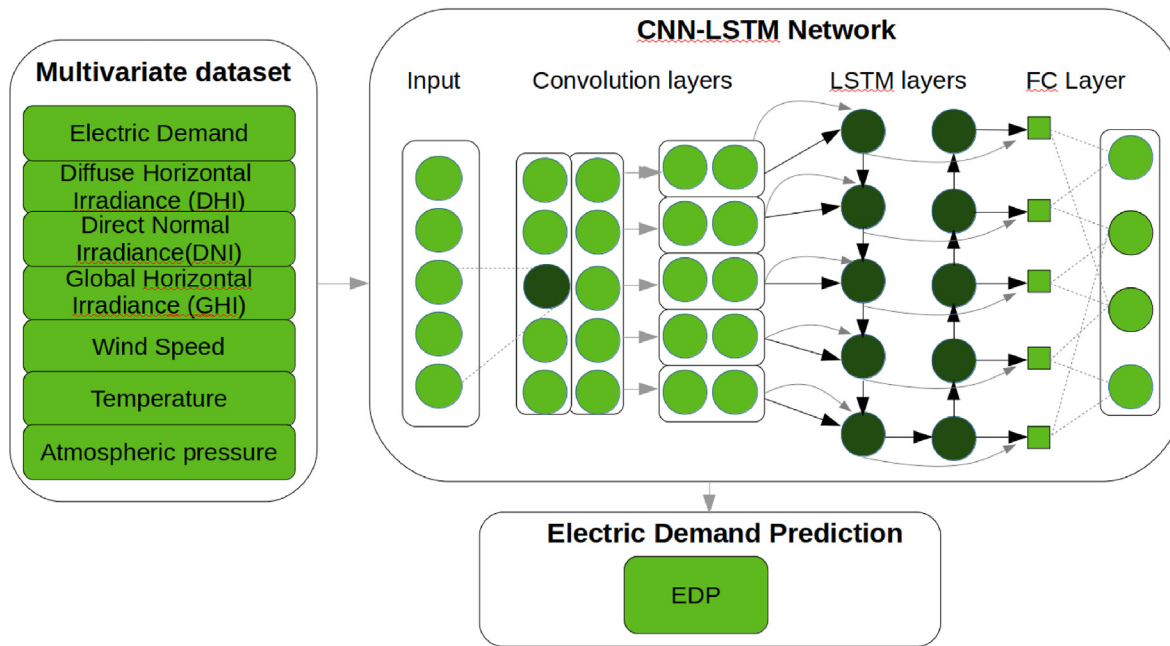


Fig. 17. The CNN-LSTM general structure for the ED model.

Table 2

Layer configuration of the proposed model.

Layer	Configuration	Activation function	
Convolution 1	filters = 64; kernel size = 3	ReLU	loss function = mse
Max-pooling 1	kernel size = 2; stride = 2		
Convolution 2	filters = 128; kernel size = 3	ReLU	optimizer = adam
Max-pooling 2	kernel size = 2; stride = 2		
Convolution 3	filters = 64; kernel size = 3	ReLU	batch size = 1
Max-pooling 3	kernel size = 2; stride = 2		
LSTM 1	Units = 64	Tanh, Sigmoid	
LSTM 2	Units = 128	Tanh, Sigmoid	
LSTM 3	Units = 64	Tanh, Sigmoid	
Dropout	dropout = 0.1		
Fully connected	Neurons = 1024		

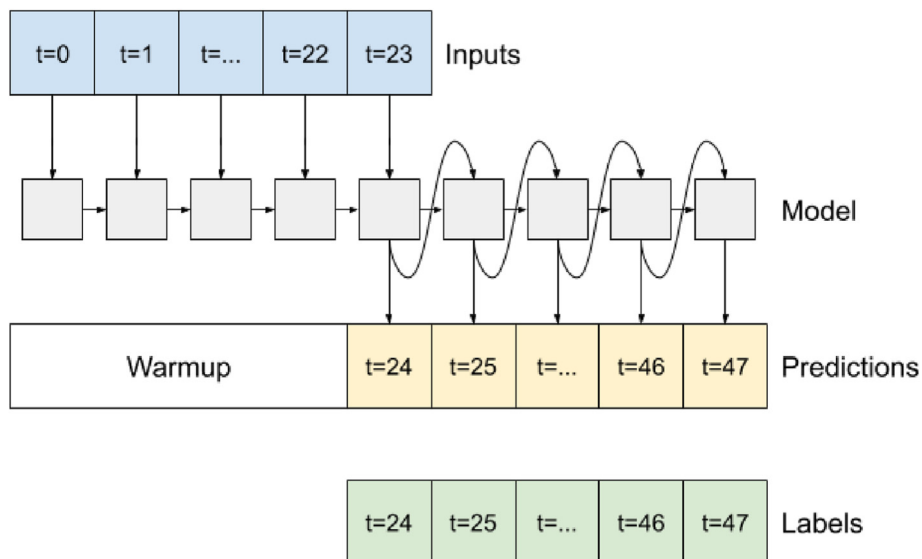


Fig. 18. Multi-step autoregressive prediction [52].

models, the results obtained by our models will be compared with a well known benchmark [53], the Autoregressive Integrated Moving Average (ARIMA) approach [54]. We will forecast PVPG, WPG and electric demand for making two different itineraries one for charging during daytime and discharging at night and the other one charging at night and discharging during the morning. These results will be further discussed in the last sections.

4.6. Performance evaluation metrics

For this work, we selected some metrics to evaluate the model. They are: MSE (Mean Square Error), RMSE (Root Mean Square Error) and MAE (Mean Absolute Error). This metrics are define as follows:

$$MSE = \frac{1}{n} \sum_{i=1}^n (\hat{Y}_i - Y_i)^2 \quad (14)$$

$$RMSE = \sqrt{\frac{1}{n} \sum_{i=1}^n (\hat{Y}_i - Y_i)^2} \quad (15)$$

$$MAE = \frac{\sum_{i=1}^n |\hat{Y}_i - Y_i|}{n} \quad (16)$$

Where Y_i are the real observed values, \hat{Y}_i refer to the predicted values and n the number of samples.

5. Results

We propose a 3D-CNN architecture with max-pooling and another 3D-LSTM structure with a fully connected layer to predict different time series data for a five days ahead horizon. We used the Keras framework and Tensorflow in Python3.6 for programming the models. The computational process was accomplished in a general purpose GPU, from the NVIDIA series with a 128-core Maxwell, and a CPU Quad-core ARM A57 (1.43 GHz).

5.1. Predictions for electric demand

As we can see in Fig. 19, the model follows the demand trend during training, with no naive behaviour such as under-fitting or

over-fitting. In Fig. 20 the prediction for electric demand for five days ahead is shown. This ED predictions will help to build the discharge time window for the itineraries in section 5.4.

In Fig. 20 the blue chart represent the true demand, the red one, the proposed hybrid CNN-LSTM model and yellow one for the ARIMA approach. As we can see for this case, the ARIMA approach underestimates the demand while the CNN-LSTM model effectively predicts the electric demand curve. We have to remark that the proposed model also underestimates this variable in some points in time; nevertheless, this error is much lower than the ARIMA approach. We can observe the temporal part is very exact and effectively predicts the two peaks. Based on this information, we will program a discharge period for the itineraries in section 5.4 from 6:00 a.m. to 13:00 p.m. (the morning peak) and other one from 22:00 p.m. to 5:00 a.m. to sheave the night time demand peak.

As it is shown in Table 3, RMSE values for the CNN-LSTM model is much lower than the ARIMA benchmark. In order to assess the forecasting result at a finer scale, a prediction of one day ahead is shown in Fig. 21, it is clear the ARIMA model has a much lower predictive effect than the proposed CNN-LSTM model for ED.

5.2. Predictions for PV power generation

The training with the machine learning technique previously discussed clearly shows there is no naive behaviour such as under-fitting or over-fitting even in rainy days. (Fig. 22).

These PVPG predictions (Fig. 23) will be used in section 5.4 to build the state of charge of an ideal BESS powered with PVPG.

As we can see in Fig. 23, both models (yellow and red) have a good predictive effect for days with high resource, but for days with low resource the prediction effect in the ARIMA model isn't as good as the CNN-LSTM, this is the case of the second and third day. In general, we can affirm that the proposed hybrid model has a better predictive effect than the ARIMA approach. Finally, we can highlight the RMSE of the hybrid CNN-LSTM model is approximately six times smaller than the ARIMA benchmark, see Table 4. In order to assess the forecasting result at a finer scale, a prediction of one day ahead is shown in Fig. 24, it is clear the ARIMA model has a minimal predictive effect in comparison with the proposed CNN-LSTM model for PVPG.

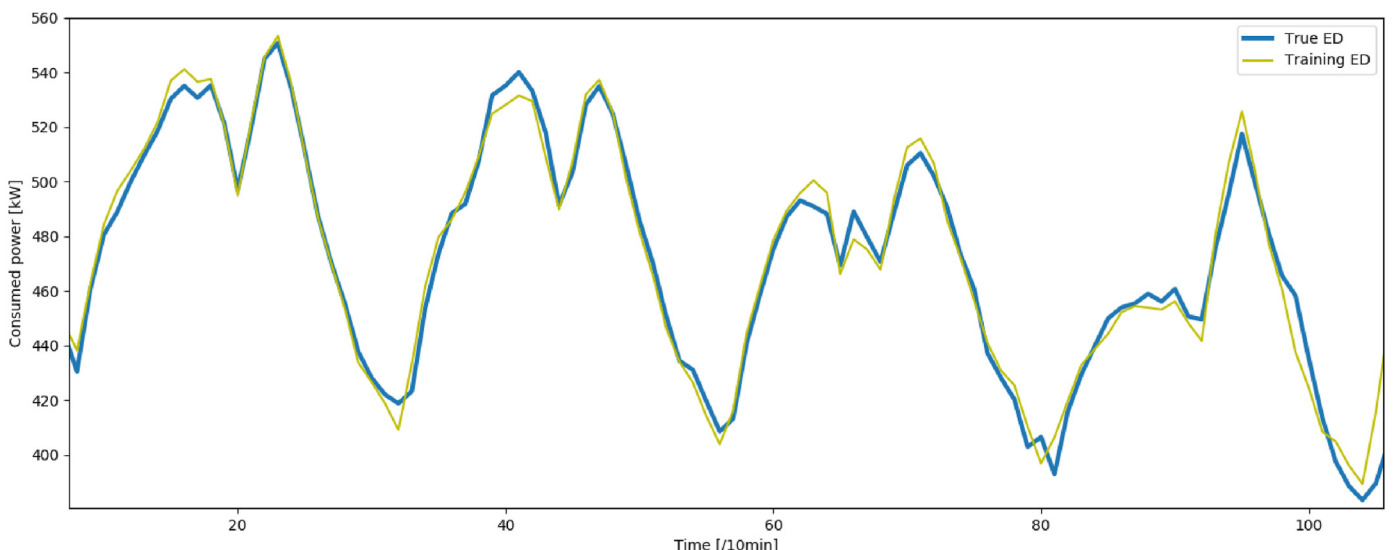


Fig. 19. Electric demand training CNN-LSTM model.

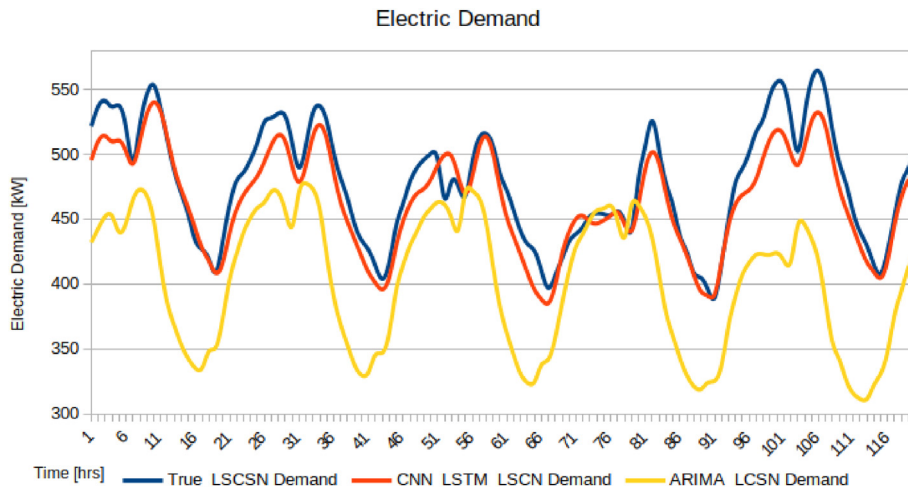


Fig. 20. Electric demand prediction for five days ahead.

Table 3
Statistic metrics comparison for the ED predictions.

Approach	MSE	RMSE	MAE
CNN LSTM 3	0.202 267	0.449 741	0.327 231
ARIMA	0.937 068	0.968 022	0.956 681

5.3. Predictions for wind generation

In Fig. 25, the training of the WPG model is shown. We can observe the hybrid model effectively follows the complex trend of wind generation with no naive behaviour such as under-fitting or over-fitting. After training the model we did a prediction for five days ahead (Fig. 26) to build a WPG-BESS state of charge with the proposed itineraries in section 5.4. As we can see, the CNN-LSTM model (red) follows the general trend of wind generation (blue). On the other hand, for this case the ARIMA approach (yellow) has a very poor predictive effect.

It is to remark the total no-fitting pattern of the ARIMA approach for the wind scenario (Fig. 26); the good performance of the hybrid neural network model for such a chaotic phenomena like wind generation is outstanding, the metrics for the two compared models is shown in Table 5. In order to assess the forecasting result

at a finer scale, a prediction of one day ahead is shown in Fig. 27, it is clear the ARIMA model has a total non-predictive effect than the proposed CNN-LSTM model for WPG.

5.4. Charge and discharge itineraries

With the presented predictions from sections 5.1 – 5.3, and the battery model presented in section 3, we built two itineraries for two ideal BESS. One powered with PVPG (Fig. 28) for attending the night-peak demand and a second ideal BESS powered with WPG (Fig. 29) for attending the morning-peak demand. We also build the real optimal itineraries based on true observations to compare the two models (CNN-LSTM and ARIMA).

To be more clear, the predictions of PVPG and WPG helped us determine when to charge each BESS and how much energy will be available for charging, either from solar and wind source, finally the ED prediction model for LCSN-BCS area, determined when to discharge these systems in order to sheave the peaks of the local demand.

As we can see in Fig. 28, both approaches work when the solar resource is available, nevertheless, for the second and third day, when the solar resource is poor the CNN-LSTM itineraries based on CNN-LSTM neural networks, work better, as we can see the error

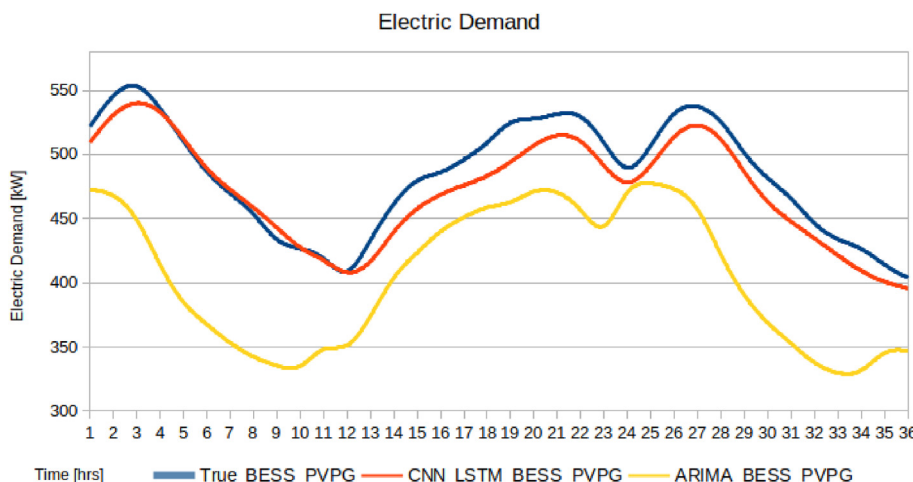


Fig. 21. Electric demand prediction for one day ahead.

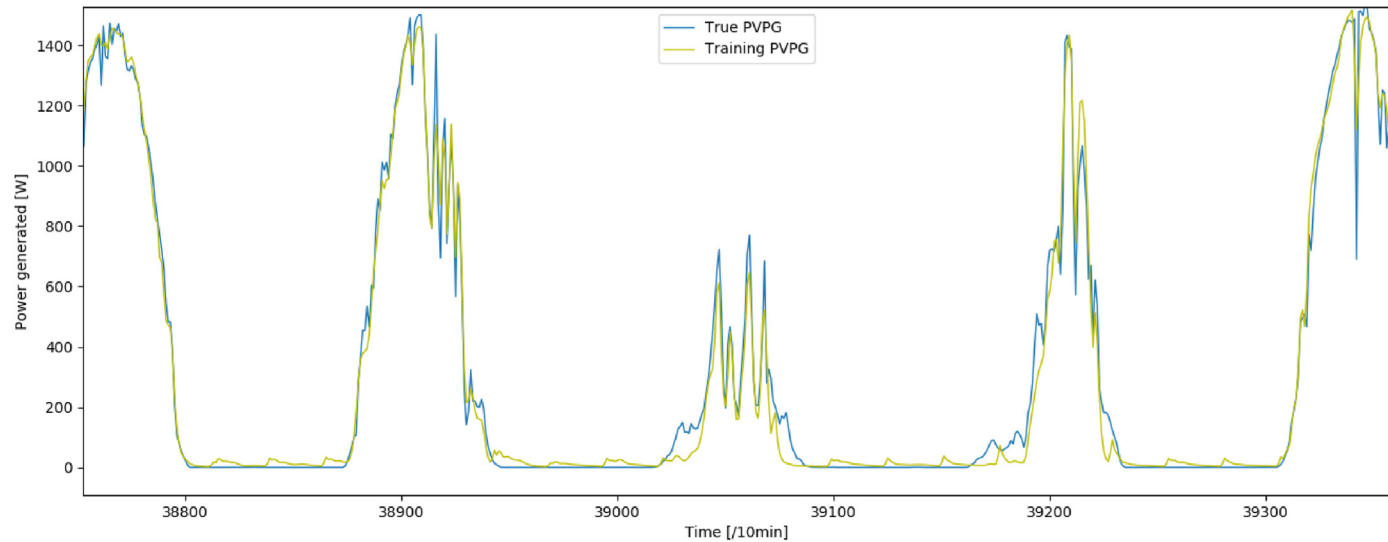


Fig. 22. PVPG training CNN-LSTM model.

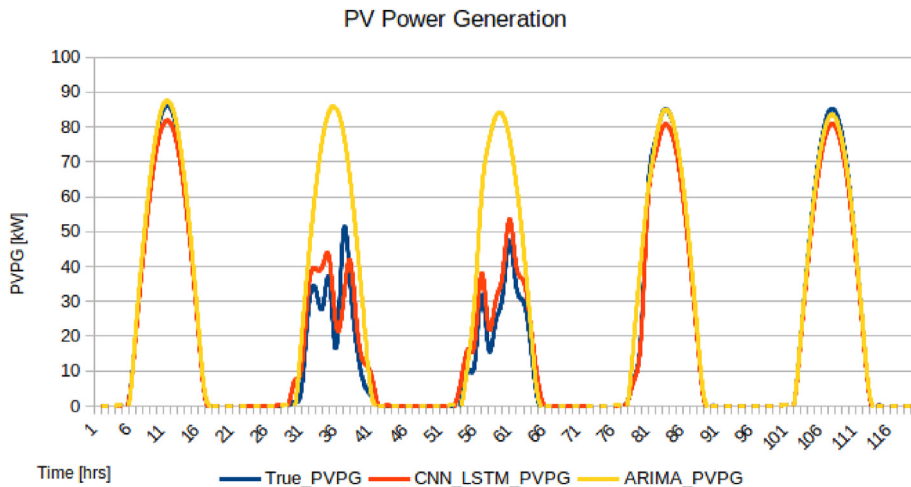


Fig. 23. PVPG prediction for five days ahead.

Table 4
Statistic metrics comparison for the PVPG predictions.

Approach	MSE	RMSE	MAE
CNN LSTM 3	0.057 184	0.239 131	0.054 413
ARIMA	0.318 736	0.564 567	0.313 131

throughout time in Fig. 30. See the metrics comparison in Table 6.

For the second BESS (Fig. 29), the ARIMA approach is not well fitted in neither of the five days; on the other hand, for the charge and discharge itineraries based on the CNN-LSTM model, we found them very accurate when the wind resource is abundant, and we register some error when the wind resource is poor (Fig. 31).

As we can observe in Table 6, the RMSE of the proposed model is approximately four times lower than the ARIMA approach for the PVPG-BESS. And for the BESS powered with WPG, a RMSE seven times lower than ARIMA (see Table 7). We found the error in the proposed model, occurs mostly in the hours with poor solar and wind resource (Figs. 30 and 31).

Thanks to the CNN-LSTM models, we were able to find an

accurate profile (in comparison with the other one based on the ARIMA benchmark), for charging the storage devices so that it will charge at the correct rate during daytime periods (PVPG-BESS), or night time periods in the WPG-BESS scenario. And discharges at the correct rate during certain period in the morning or in the evening in order to sheave the demand peaks. With this new method we intend to provide reliability of solar or wind generation, which is one of the most criticized issues of these variant sources [55].

Finally, we experimented with a finer scale and with different time prediction horizons for the itineraries, see Table 8. These results show a RMSE for the proposed model to be lower than a single layer LSTM model; but must important, lower than the competitive benchmark ARIMA in all cases (see Table 8 and Fig. 32).

5.5. Peak shaving with itineraries of an ideal BESS based on CNN-LSTM predictions for Los Cabos San Lucas, BCS

As we explained in section 1.2, peak shaving in a scenario with BESS powered by REG, can reduce the usage of conventional power plants, which often use fossil fuels, like in the case of the BCS's electrical grid. Also the usage of these electric power plants are

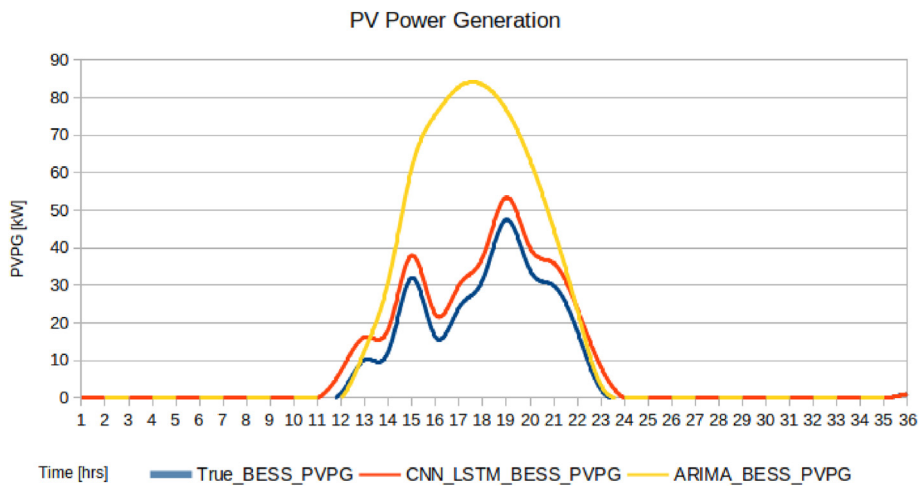


Fig. 24. PVPG prediction for a single day.

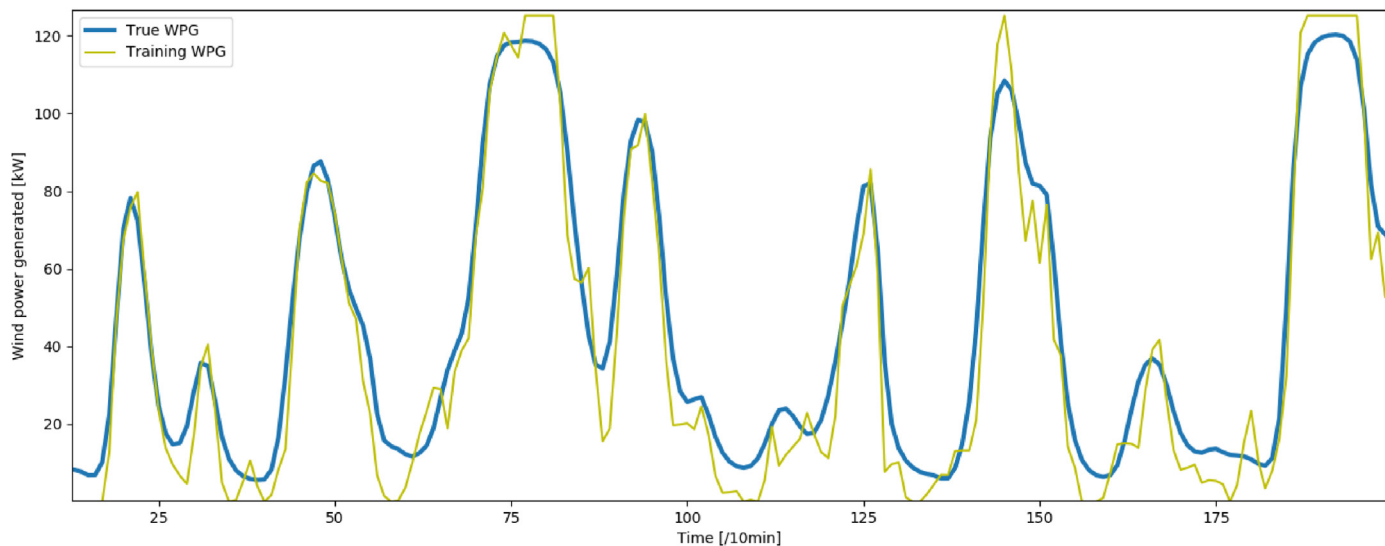


Fig. 25. WPG training CNN-LSTM model.

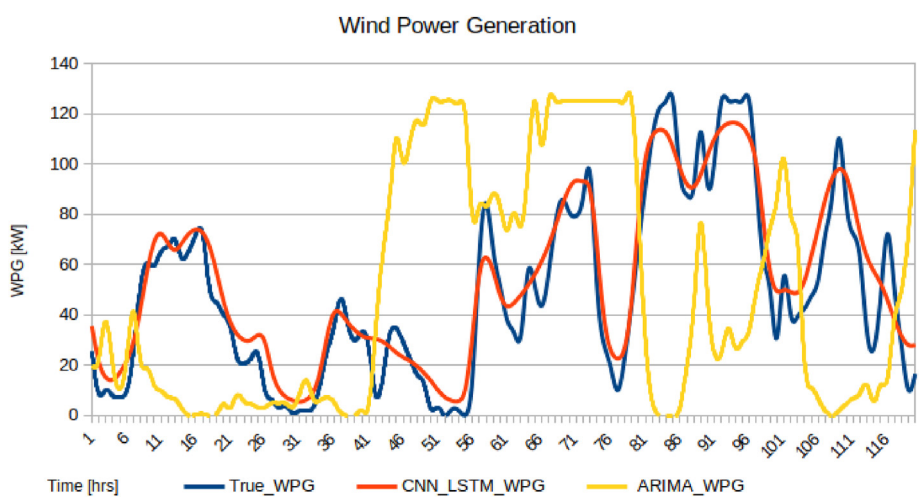


Fig. 26. WPG prediction for five days ahead.

Table 5

Statistic metrics comparison for the WPG predictions.

Approach	MSE	RMSE	MAE
CNN LSTM 3	0.116 356	0.341 109	0.102 273
ARIMA	4.278 693	2.068 500	4.018 773

expensive due to the isolation of the region [7,42,50].

The usage of itineraries of charge and discharge with a data based approach, show a better performance for predicting when to charge and when to discharge the energy from intermittent sources, compared with other well known benchmarks, see Figs. 28 and 29.

Finally, in this last section we present the effect of the two ideal BESS in the two peaks of the studied area, (Figs. 33 and 34). As expected, the days with less resource have less effect than the days when the resource is abundant. Note the first day the BESSs had no effect because we assume we start the battery systems fully discharged.

Also we need to highlight that in some cases not only the BESS was injected but also surplus energy, in the case of WPG-BESS for example, in days 4 and 5, the wind resource was so abundant in the time window of the second peak, that the reduction of it was

outstanding, see Fig. 34.

Fig. 35 shows the effect of the two BESS based on itineraries with a neural network prediction approach. For this work we assume the two ideal BESS are totally discharged that's why in the first day there is a minimal effect on the demand. Nevertheless, for the next 4 days we can observe the optimized demand values doesn't exceed 490 – 450[kW].

6. Conclusion

In this work we presented an application for energy time series predictions (demand and generation), to increase penetrability of renewable generation with intelligent itineraries of charge and discharge of two ideal BESS.

We presented the case of BCS in the location of Los Cabos San Lucas because solar and wind resource in the region is abundant [9]. We used available weather and electric demand data for the region of LCSN-BCS, to train a hybrid CNN-LSTM neural network model, the predictions of PVPG and WPG helped us to know when to charge each BESS. And the ED CNN-LSTM model helped us to know when the peak will occur and therefore discharge the energy from REG. In other words, the purpose of the BESS model is to maximise the morning and evening peak reduction for the demand

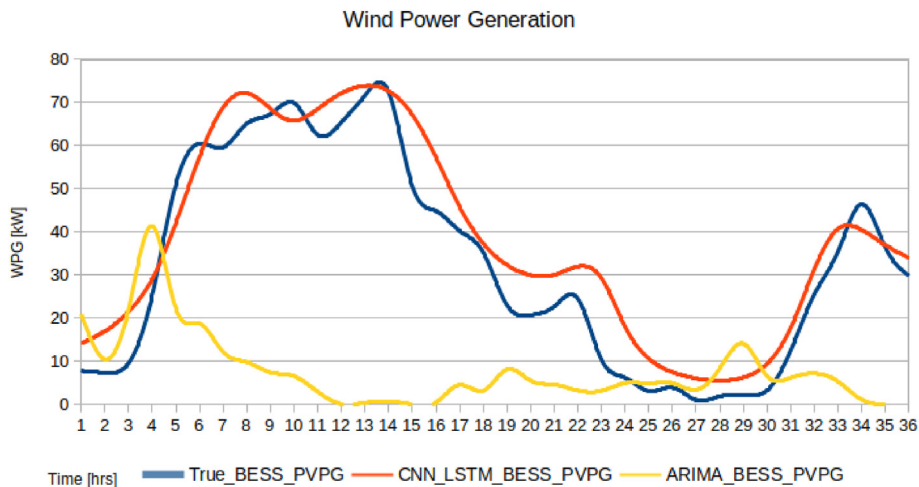


Fig. 27. WPG prediction for a single day.

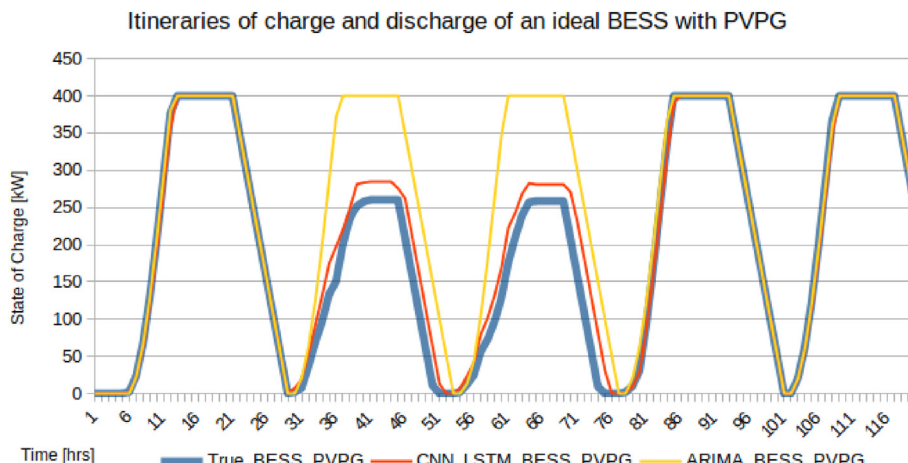


Fig. 28. Itineraries of charge and discharge for the PV-BESS.

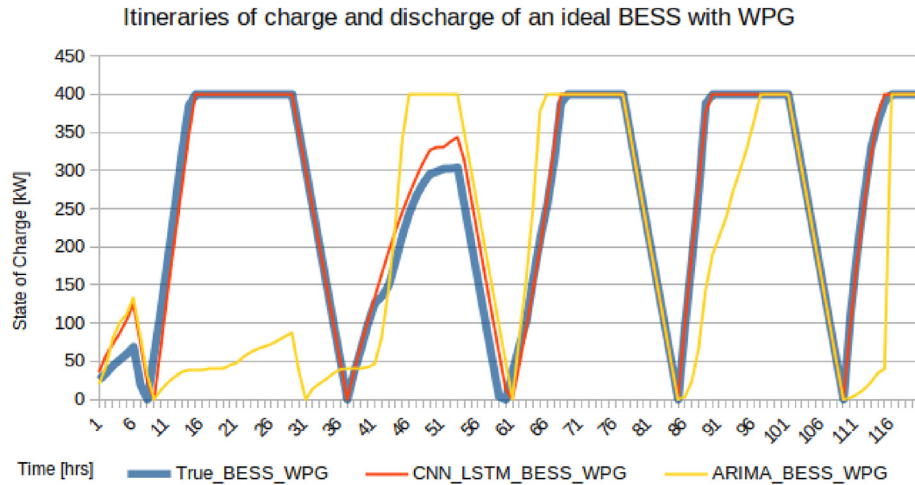


Fig. 29. Itineraries of charge and discharge for the WPG-BESS.

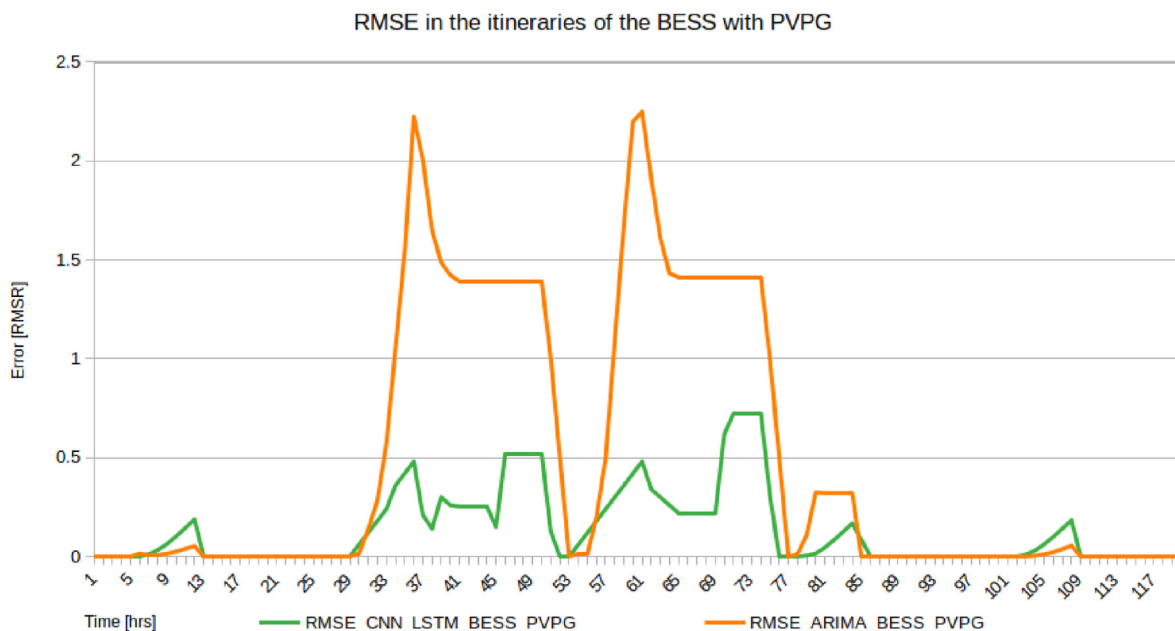


Fig. 30. RMSE throughout 5 days for the PVPG-BESS itineraries.

Table 6
Statistic metrics comparison for the PVPG-BESS itineraries.

Approach	MSE	RMSE	MAE
CNN LSTM 3	0.174 132	0.417 291	0.112 337
ARIMA	0.748 722	0.865 287	0.706 894

with two distribution feeders for each day, over a five days period whilst utilising as much solar PVPG or WPG as possible to do so.

This is done by finding an appropriate charging profile for the storage device so that it charges at the correct rate during daytime periods (or night time periods) when there is high solar or wind generation, and discharges at the correct rate during certain period in the morning or in the evening.

The results show a higher accuracy for itineraries based on hybrid neural networks, compared with itineraries based on a well known benchmark. For the BESS power by PVPG, we found the error (RMSE) is approximately 4 times lower than the ARIMA

approach (Table 6). And approximately 6 times a lower error for the BESS powered by WPG (Table 7).

For the solar and the wind cases (Figs. 28 and 29), we found that the days when resource is poor and with high intermittent behaviour, the itineraries with the hybrid neural approach performed better than ARIMA based itineraries (Figs. 30 and 31). The good predictability performance of the itineraries based on hybrid neural networks will be able to increase energy reliability and therefore penetration of renewable intermittent sources.

We also experimented with a finer scale and with different time prediction horizons for the itineraries (10 min, 30 min, 60 min, 90 min, 120 min, 150 min and 180 min). These results show the RMSE of the proposed model to be lower than the ARIMA competitive benchmark and a single layer LSTM neural network in all cases (see Table 8 and Fig. 32).

We need to remark that the presented model for the BESS is an idealization, further studies need to incorporate a more realistic model that consider battery materials, state of the battery life, etc.

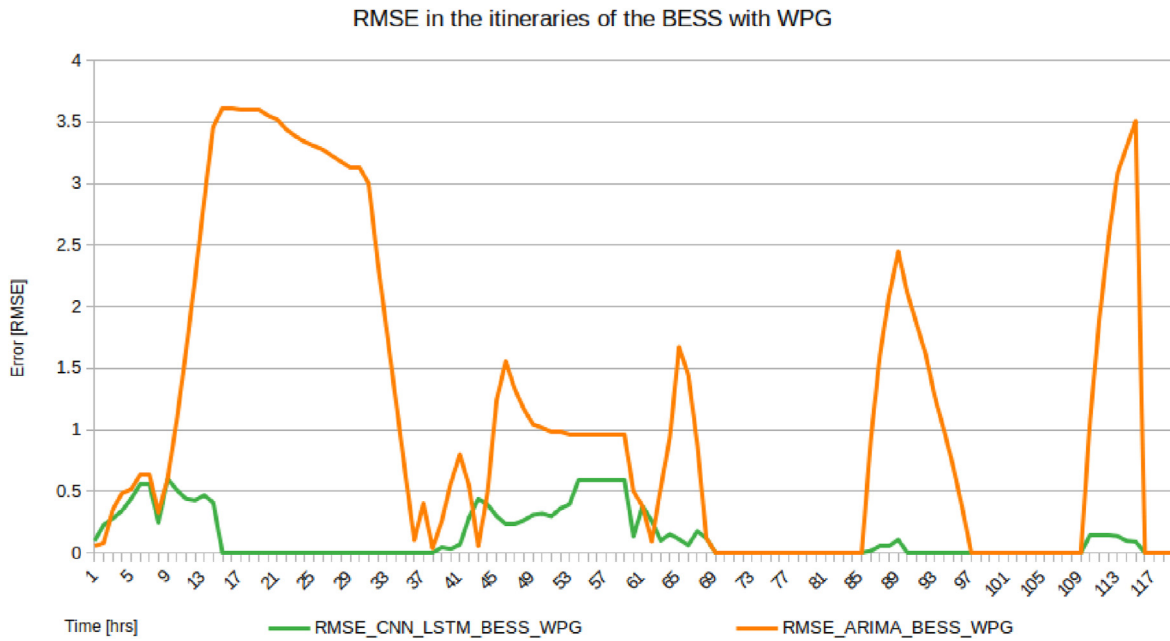


Fig. 31. RMSE throughout 5 days for the WPG-BESS itineraries.

Table 7
Statistic metrics comparison for the WPG-BESS itineraries.

Approach	MSE	RMSE	MAE
CNN LSTM 3	0.218 728	0.467 684	0.195 587
ARIMA	4.818 722	2.133 484	4.317 960

Also, we presented the peak shaving effect of the proposed itineraries based on hybrid neural networks in the local electric demand Fig. 35 of LCSN-BCS. We believe the implementation of this strategy for prosumers (users that consume and produce electricity) in micro-grids (MG's) scenarios, will have a positive effect for the general electric distribution grid in a location [47], but further studies need to be made.

7. Future work

New advances in machine learning techniques such as attention mechanisms [44] or neural Ordinary Differential Equations (ODE's) networks [56], etc. These novel models aim to increase precision and memory efficiency in time series forecasting. Other techniques like reinforcement learning [57] should be studied to incorporate them in prediction models.

Also, new approaches such as fuzzy logic [58] or elastic net regularization [49] have achieved outstanding results in energy management and decision making in MG's. The performance of these models, with hybrid deep neural networks models should be compared and studied in detail.

The study of continuous, light and memory efficient models such as neural ODE's [56] should be addressed. As well, the incorporation of low cost general purpose GPU's (such as Jetson NVIDIA series) in MG's with REG, will increase reliability, by giving the prosumer a powerful tool to learn different spacial and temporal features of different time series data such as demand and local generation.

Table 8
Performance comparison of the proposed method with ARIMA.

Approach	MSE	RMSE	MAE
CNN-LSTM-3	0.005 766	0.075 935	0.005 248
LSTM	0.082 337	0.286 944	0.081 326
ARIMA	0.109 811	0.331 377	0.131 796
<i>Prediction horizon = 10 min</i>			
Approach	MSE	RMSE	MAE
CNN-LSTM-3	0.008 649 3	0.093 001 6	0.008 132
LSTM	0.123 506 1	0.351 434 3	0.136 268 5
ARIMA	0.264 716 5	0.514 506 0	0.231 796 0
<i>Prediction horizon = 30 min</i>			
Approach	MSE	RMSE	MAE
CNN-LSTM-3	0.023 353 11	0.152 817 2	0.021 097 7
LSTM	0.185 259 15	0.430 417 41	0.171 683 3
ARIMA	0.444 734 5	0.666 884 21	0.421 027 4
<i>Prediction horizon = 60 min</i>			
Approach	MSE	RMSE	MAE
CNN-LSTM-3	0.063 053 397	0.251 104 3	1.313 268
LSTM	0.277 888 725	0.527 151 5	0.310 661
ARIMA	0.651 287 61	0.807 023 9	0.619 982
<i>Prediction horizon = 90 min</i>			
Approach	MSE	RMSE	MAE
CNN-LSTM-3	0.097 722 8	0.312 606 5	0.106 811 1
LSTM	0.416 833 087 5	0.645 626 1	0.443 303
ARIMA	0.892 416 371	0.944 677 9	0.867 188 8
<i>Prediction horizon = 120 min</i>			
Approach	MSE	RMSE	MAE
CNN-LSTM-3	0.159 772 8	0.399 715 9	0.151 428 0
LSTM	0.625 249 6	0.790 727 2	0.602 142 1
ARIMA	1.417 972 6	1.190 786 5	1.477 236 8
<i>Prediction horizon = 150 min</i>			
Approach	MSE	RMSE	MAE
CNN-LSTM-3	0.226 066 2	0.475 464 2	0.262 096 1
LSTM	0.937 874 4	0.968 439 1	0.900 429 5
ARIMA	1.936 152 8	1.391 457 1	1.921 515
<i>Prediction horizon = 180 min</i>			

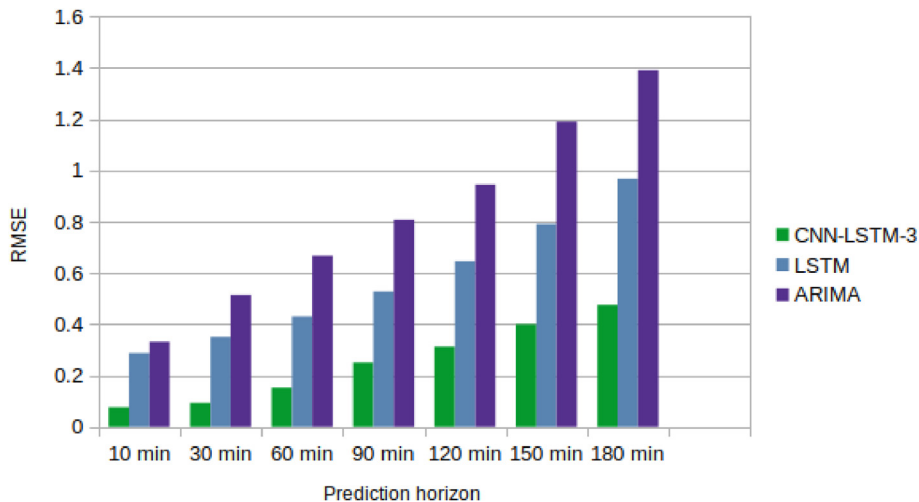


Fig. 32. RMSE performance comparison of the proposed approach with ARIMA and a single layer LSTM model.

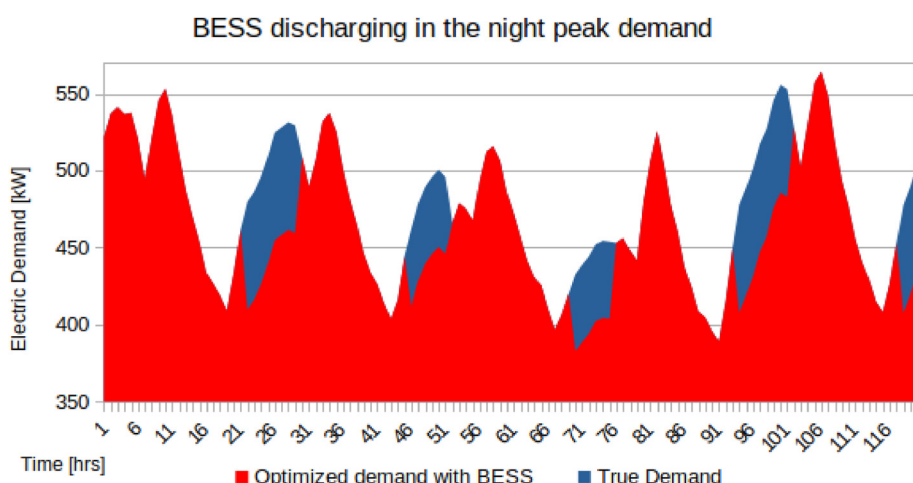


Fig. 33. Peak shaving at night with PVPG-BESS itineraries.

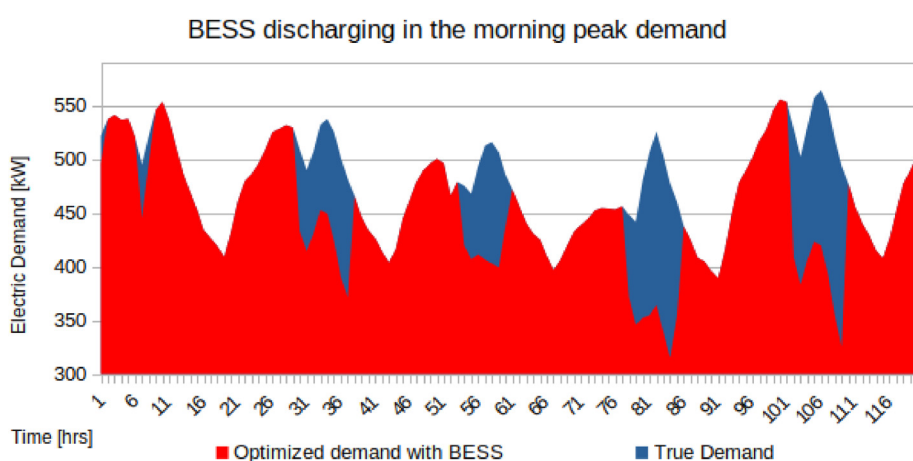


Fig. 34. Peak shaving in the morning with WPG-BESS itineraries.

CRedit authorship contribution statement

Mario A. Tovar Rosas: Term, Conceptualization, Methodology,

Software, Validation, Formal analysis, Investigation, Resources, Data curation, Writing – original draft, Writing – review & editing, Visualization, Project administration. **Miguel Robles Pérez:**

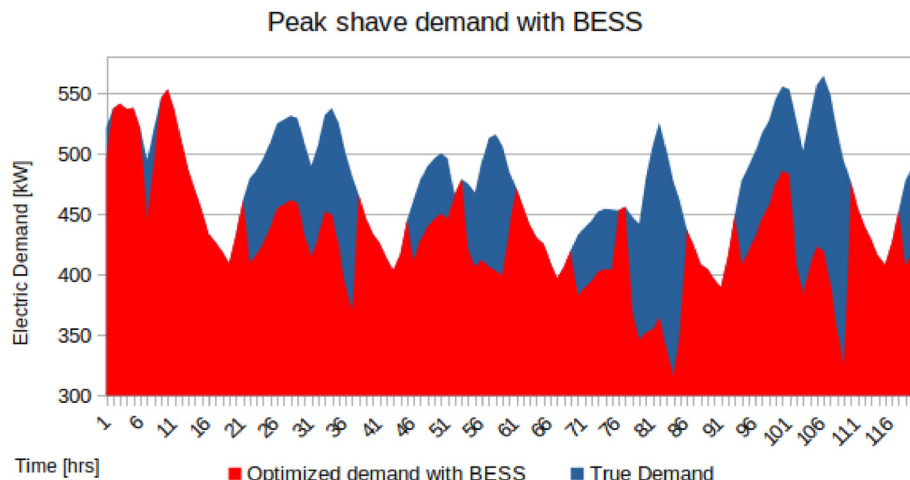


Fig. 35. Peak shaving in the morning and night time with PVPG-BESS and WPG-BESS itineraries.

Validation, Resources, Writing – review & editing, Supervision, Funding acquisition. **E. Rafael Martínez Pérez:** Software, Validation.

Declaration of competing interest

The authors declare that they have no known competing financial interests or personal relationships that could have appeared to influence the work reported in this paper.

Acknowledgements

This work was supported by the National Council of Science and Technology of México (CONACYT), the equipment of the Renewable Energy Institute of the National University of Mexico (IER - UNAM) and the Science Faculty (FC-UNAM).

Abbreviations. The following abbreviations are used in this manuscript

ARIMA	Autoregressive Integrated Moving Average
ANN	Artificial Neural Network
BCS	Baja California Sur
BESS	Battery Energy Storage System
CAES	Compressed Air Energy Storage
CENACE	Centro Nacional de Control de Energía
CNN	Convolutional Neural Network
CONACyT	Consejo Nacional de Ciencia y Tecnología
CPU	Central Processing Unit
DG	Distributed Generation
DHI	Diffuse Horizontal Irradiance
DNI	Direct Normal Irradiance
ED	Electric demand
EESS	Electric Energy Storage System
ESS	Energy Storage System
FC	Facultad de Ciencias - UNAM
GHI	Global Horizontal Irradiance
GPU	Graphic Processing Unit
IER	Instituto de Energías Renovables
LCSN	Los Cabos San Lucas
LSTM	Long-Short Term Memory
MAE	Mean Absolute Error
MG's	Microgrids
MSE	Mean Square Error

NREL	National Renewable Energy Laboratory
ODE	Ordinary Differential Equation
PV	Photo Voltaic
PVPG	Photo Voltaic Power Generation
RE	Renewable Energy
REG	Renewable Energy Generation
ReLU	Rectified Linear Unit
RMSE	Root Mean Square Error
RNN	Recurrent Neural Network
SAM	System Advisor Model
SPG	System Power Generated
UNAM	Universidad Nacional Autónoma de México
WPG	Wind Power Generation

References

- [1] Huangjie Gong, Vandana Rallabandi, Michael L. McIntyre, Eklas Hossain, M. Dan, Ionel, Peak reduction and long term load forecasting for large residential communities including smart homes with energy storage, *IEEE Access* 9 (2021) 19345–19355.
- [2] Hyung Jun Moon, Seok Jun Bu, Sung Bae Cho, Learning disentangled representation of residential power demand peak via convolutional-recurrent triplet network, *IEEE Int. Conf. Data. Mining. Workshop, ICDMW* (2020) 757–761. 2020-Novem.
- [3] Sternkopf Benjamin, Pesnel Pierre, Electrical energy storage in Mexico, *Deutsche Gesellschaft für Internationale Zusammenarbeit (GIZ)* 1 (2019) 6–12.
- [4] Christoph Heilmann, David Wozabal, How much smart charging is smart? *Appl. Energy* 291 (February) (2021), 116813.
- [5] Kou Peng, Deliang Liang, Lin Gao, Distributed EMPC of Multiple Microgrids for Coordinated Stochastic Energy Management, *Applied Energy*, 2016.
- [6] Huai Su, Lixun Chi, Enrico Zio, Zhenlin Li, Lin Fan, Zhe Yang, Zhe Liu, Jinjun Zhang, An integrated, systematic data-driven supply-demand side management method for smart integrated energy systems, *Energy* 235 (2021), 121416.
- [7] Comisión Federal de Electricidad (CFE), Estadísticas por regiones de transmisión, Mexico, Available:, Consulted: March 2021, http://www.cfe.gob.mx/ConoceCFE/1_AcercaCFE/Estadisticas/.
- [8] Secretaría de Energía (SENER-SIE), Sistema de información energética, estadísticas energéticas nacionales, Mexico, 2018. Consulted: February 2021, <http://sie.energia.gob.mx/>. Available:.
- [9] Carlo Brancucci Martinez-Anido, Renewable integration study baja California sur (baja-ris), in: 21st CPP Steering Committee Meeting, Ciudad de México, 27 de Septiembre del 2016.
- [10] Robert Blaga, Andreea Sabadus, Nicoleta Stefu, Ciprian Dughir, Marius Paulescu, A current perspective on the accuracy of incoming solar energy forecasting, *Prog. Energy Combust. Sci.* 70 (2019) 119–144.
- [11] Reihaneh Haji, Mahdizadeh Zargar, Mohammad Hossein Yaghmaee, Senior Member, Development of a Markov-Chain-Based Solar Generation Model for Smart Microgrid Energy Management System, vol. 3029, 2019 c.
- [12] Min Gao, Kun Wang, A Continuous-time Markov Chain, Probabilistic Model Checking for Green Energy Router System in Energy Internet, 2017.
- [13] Cyril Voyant, Gilles Notton, Soteris Kalogirou, Marie-laure Nivet,

- Christophe Paoli, Fabrice Motte, Alexis Fouilloy, Machine learning methods for solar radiation forecasting : a review, *Renew. Energy* 105 (2017) 569–582.
- [14] Shawn A. Chandler, Joshua G. Hughes, Smart Grid Distribution Prediction and Control Using Computational Intelligence, 2013, pp. 86–89.
- [15] Pilar Gómez-Gil, Juan Manuel Ramírez-Cortes, E. Saúl, Pomares Hernández, Vicente Alarcón-Aquino, A neural network scheme for long-term forecasting of chaotic time series, *Neural Process. Lett.* 33 (3) (2011) 215–233.
- [16] Mohamed Abdel-Nasser, Karar Mahmoud, Accurate photovoltaic power forecasting models using deep LSTM-RNN, *Neural Comput. Appl.* 31 (7) (2019) 2727–2740.
- [17] Ba Ümmühan, Tansu Filik, Wind Speed Prediction Using Artificial Neural Networks Based on Multiple Local Measurements in Eskisehir, vol. 107, 2017, pp. 264–269, September 2016.
- [18] Zhuyi Rao, Yunxiang Zhang, Transformer-based power system energy prediction model, in: Proceedings of 2020 IEEE 5th Information Technology and Mechatronics Engineering Conference, ITOEC, 2020, pp. 913–917, 2020, (Itoec).
- [19] Tuong Le, Minh Thanh Vo, Bay Vo, Eenjun Hwang, and Seungmin Rho, Applied Sciences Improving Electric Energy Consumption Prediction.
- [20] K. Muralitharan, R. Sakthivel, R. Vishnuvarthan, Neural Network Based Optimization Approach for Energy Demand Prediction in Smart Grid AC PT US CR, *Neurocomputing*, 2017.
- [21] Yaguang Li, Rose Yu, Cyrus Shahabi, Yan Liu, Diffusion convolutional recurrent neural network: data-driven traffic forecasting, in: 6th International Conference on Learning Representations, ICLR 2018 - Conference Track Proceedings, 2018, pp. 1–16.
- [22] Power Predictions, Extreme Learning Machines for Solar Photovoltaic Updated the, Figure 1), 2018.
- [23] Xi Fang, Guangcui Gong, Guannan Li, Liang Chun, Pei Peng, Wenqiang Li, A general multi-source ensemble transfer learning framework integrate of LSTM-DANN and similarity metric for building energy prediction, *Energy Build.* 252 (2021), 111435.
- [24] Qicheng Tang, Mengning Yang, ST-LSTM : A Deep Learning Approach Combined Spatio-Temporal Features for Short-Term Forecast in Rail Transit. 2019, 2019.
- [25] Malvern Madondo, Thomas Gibbons, Learning and modeling chaos using LSTM recurrent neural networks, in: Proceedings of the Midwest Instruction and Computing Symposium, 2018.
- [26] Ling Zheng, Bin Zhou, Wing Or Siu, Yijia Cao, Huaizhi Wang, Yong Li, Ka Wing Chan, Spatio-temporal wind speed prediction of multiple wind farms using capsule network, *Renew. Energy* 175 (2021) 718–730.
- [27] Antonello Rosato, Rodolfo Araneo, Amedeo Andreotti, Federico Succetti, Massimo Panella, 2-D convolutional deep neural network for the multivariate prediction of photovoltaic time series, *Energies* 14 (9) (2021) 1–18.
- [28] Wei Li, Denis Mike Becker, Day-ahead electricity price prediction applying hybrid models of LSTM-based deep learning methods and feature selection algorithms under consideration of market coupling, *Energy* 237 (2021), 121543.
- [29] Musaed Alhussein, Khursheed Aurangzeb, Syed Irtaza Haider, Hybrid CNN-LSTM model for short-term individual household load forecasting, *IEEE Access* 8 (2020) 180544–180557.
- [30] Ayush Sinha, Raghav Tayal, Aamod Vyas, Pankaj Pandey, O.P. Vyas, Forecasting electricity load with hybrid scalable model based on stacked non linear residual approach, *Front. Energy Res.* 9 (November) (2021) 1–17.
- [31] Tae-young Kim, Sung-bae Cho, Predicting residential energy consumption using CNN-LSTM neural networks, *Energy* 182 (2019) 72–81.
- [32] Jiaqi Qin, Yi Zhang, Shixiong Fan, Xiaonan Hu, Yongqiang Huang, Zexin Lu, Yan Liu, Multi-task short-term reactive and active load forecasting method based on attention-LSTM model, *Int. J. Electr. Power Energy Syst.* 135 (August 2021) (2022), 107517.
- [33] Simran Kaur Hora, Rachana Poongodan, Rocío Pérez de Prado, Marcin Woźniak, Parameshchari Bidare Divakarachari, Long short-term memory network-based metaheuristic for effective electric energy consumption prediction, *Appl. Sci.* 11 (23) (2021).
- [34] Kejun Wang, Xiaoxia Qi, Hongda Liu, Photovoltaic power forecasting based LSTM-Convolutional Network, *Energy* 189 (2019), 116225.
- [35] M. Tovar, F. Rashid, M. Robles, PV Power Prediction, Using CNN-LSTM Hybrid Neural Network Model. Case of Study: Temixco-Morelos, México, MDPI Energies, 2020.
- [36] Bixuan Gao, Xiaoqiao Huang, Junsheng Shi, Yonghang Tai, Jun Zhang, Hourly forecasting of solar irradiance based on CEEMDAN and multi-strategy CNN-LSTM neural networks, *Renew. Energy* 162 (2020) 1665–1683.
- [37] Dazhi Yang, A guideline to solar forecasting research practice: reproducible, operational, probabilistic or physically-based, ensemble, and skill (ROPEs), *J. Renew. Sustain. Energy* 11 (2) (2019).
- [38] Tomoharu Iwata, Atsutoshi Kumagai, Few-shot Learning for Time-Series Forecasting, 2020, pp. 1–10.
- [39] Junseo Son, Yongtae Park, Junu Lee, Hyogon Kim, Sensorless PV power forecasting in grid-connected buildings through deep learning, *Sensors (Switzerland)* 18 (8) (aug 2018).
- [40] Ioannis Mexis, Grazia Todeschini, Battery energy storage systems in the United Kingdom: a review of current state-of-the-art and future applications, *Energies* 13 (14) (2020).
- [41] S. B. T. Y., & Cho, Predicting residential energy consumption using cnn-lstm neural networks, *Energy* 182 (2019).
- [42] Centro Nacional de Control de Energía (CENACE), Diagramas unifilares del sistema eléctrico nacional 2016 – 2021, Consulted: November 2020, *Programa de Ampliación y Modernización 2016 - 2030*, <http://www.cenace.gob.mx/Docs/MercadoOperacion/ModGralPlaneacion/Mod%20Gral%20Planeaci%C3%B3n%2020162021%20Diagramas%20Unifilares%20RNT%20y%20RGD%20de%20MEM.pdf>. Available:.
- [43] Bibi Ibrahim, Luis Rabelo, A deep learning approach for peak load forecasting: a case study on Panama, *Energies* 14 (11) (2021).
- [44] Marija Žima-Bockarjova, Antans Sauhats, Lubov Petrichenko, Petrichenko Roman, Charging and discharging scheduling for electrical vehicles using a shapley-value approach, *Energies* 13 (5) (2020) 1–21.
- [45] National Renewable Energy Laboratory, Solar Power Data for Integration Studies, Consulted: September, 2020, NREL, 2020. Available: <https://www.nrel.gov/grid/solar-power-data.html>.
- [46] SAM NREL System Advisor Model. NREL Software, Available: <https://sam.nrel.gov/>, Consulted: May 2021.
- [47] Esther Mengelkamp, Kessler Scott, Johannes Gärtner, Kerstin Rock, Lawrence Orsini, Christof Weinhardt, Designing microgrid energy markets, *Appl. Energy* 210 (2017) 870–880.
- [48] Andrea Monacchi, Wilfried Elmreich, Assisted energy management in smart microgrids, *J. Ambient Intell. Hum. Comput.* 7 (6) (2016) 901–913.
- [49] Antonello Rosato, Massimo Panella, Amedeo Andreotti, Osama A. Mohammed, Rodolfo Araneo, Two-stage dynamic management in energy communities using a decision system based on elastic net regularization, *Appl. Energy* 291 (February) (2021), 116852.
- [50] Comisión Reguladora de Energía (CRE), Generación Distribuida (Gd), Published: April 4th, 2017. Consulted: June 2021, México, Available: <https://www.gob.mx/cre/articulos/generacion-distribuida-102284>.
- [51] Jeff Donahue, Lisa Anne Hendricks, Sergio Guadarrama, Marcus Rohrbach, Subhashini Venugopalan, Kate Saenko, Trevor Darrell, U.T. Austin, UMass Lowell, U.C. Berkeley, Long-term Recurrent Convolutional Networks for Visual Recognition and Description, 2015, pp. 2625–2634.
- [52] Tensorflow, Time Series Forecasting. Advanced Autoregressive Model, Consulted: January, 2022, 2022. Available: https://www.tensorflow.org/tutorials/structured_data/time_series#advanced_autoregressive_model.
- [53] Hugo T.C. Pedro, David P. Larson, Carlos F.M. Coimbra, A comprehensive dataset for the accelerated development and benchmarking of solar forecasting methods, *J. Renew. Sustain. Energy* 11 (3) (2019).
- [54] Arpad Gellert, Ugo Fiore, Adrian Florea, Chis Radu, Francesco Palmieri, Forecasting electricity consumption and production in smart homes through statistical methods, *Sustain. Cities Soc.* 76 (April 2021) (2022), 103426.
- [55] Tiago Pinto, Mohammad Ali Fotouhi Ghazvini, Joao Soares, Ricardo Faia, Juan Manuel Corchado, Rui Castro, Zita Vale, Decision support for negotiations among microgrids using a multiagent architecture, *Energies* 11 (10) (2018).
- [56] Ricky T. Q. Chen, Yulia Rubanova, Jesse Bettencourt, and David Duvenaud, Neural Ordinary Differential Equations, NeurIPS, 2nd Conference on Neural Information Processing Systems (NeurIPS 2018), Montréal, Canada.
- [57] David Domínguez-Barbero, Javier García-González, Miguel A. Sanz-Bobi, Eugenio F. Sánchez-Úbeda, Optimising a microgrid system by deep reinforcement learning techniques, *Energies* 13 (11) (2020).
- [58] Stefano Leonori, Enrico De Santis, Antonello Rizzi, F.M. Frattale Mascioli, Optimization of a microgrid energy management system based on a Fuzzy Logic Controller, IECON Proceedings (Industrial Electronics Conference) (2016) 6615–6620.